



Universidade de Aveiro
2020

Departamento de Química

**Miguel
Godinho de
Oliveira Anjos**

**O efeito da doxorubicina e do
trastuzumab na remodelação molecular
do músculo estriado**

**The impact of doxorubicin and
trastuzumab on the molecular remodeling
of striated muscle**



Universidade de Aveiro
2020

Departamento de Química

**Miguel
Godinho de
Oliveira Anjos**

**O efeito da doxorrubicina e do
trastuzumab na remodelação molecular do
músculo estriado**

**The impact of doxorubicin and
trastuzumab on the molecular remodeling
of striated muscle**

Dissertação apresentada à Universidade de Aveiro para cumprimento dos requisitos necessários à obtenção do grau de Mestre em Bioquímica, realizada sob a orientação científica da Doutora Rita Ferreira, Professora Auxiliar do Departamento de Química da Universidade de Aveiro, e do Doutor Mário Santos, Assistente Hospitalar de Cardiologia no Centro Hospitalar Universitário do Porto – Hospital de Santo António.

Apoio financeiro de fundos de Investimento Europeus FEDER/COMPETE/POCI – *Operational Competitiveness and Internationalisation Programme* – e fundo da FCT – Fundação para a Ciência e Tecnologia – ao projeto PTDC/DTP-FTO/1489/2014 – POCI-01-0145-FEDER-016537 e às unidades de investigação LAQV (UIDB/50006/2020) e UMIB (PEst-OE/SAU/UI0215/2019).

Dedico este trabalho à minha família.

o júri

presidente

Doutor Brian James Goodfellow

Professor Assistente do Departamento de Química da Universidade de Aveiro

Doutora Rita Maria Pinho Ferreira

Professora Auxiliar do Departamento de Química da Universidade de Aveiro

Doutor Daniel Moreira Gonçalves

Professor Auxiliar da Faculdade de Desporto da Universidade do Porto

agradecimentos

Em primeiro lugar, um reconhecimento especial à minha orientadora, a Professora Rita Ferreira, pela disponibilidade, apoio incondicional e sugestões que foram essenciais, quer para aumentar o meu conhecimento científico e laboratorial, quer para a concretização desta dissertação.

Ao meu coorientador, o Doutor Mário Santos, as sugestões que foram importantes para aperfeiçoar o meu trabalho.

À técnica de laboratório, Cristina Barros, agradeço a disponibilidade e simpatia em todos os momentos que necessitei de ajuda.

Às alunas de doutoramento, Sofia Brandão e Alexandra Pais, pelos conhecimentos laboratoriais que me transmitiram e pela disponibilidade na ajuda das dúvidas colocadas.

palavras-chave

Cardiotoxicidade; Doxorrubicina; Trastuzumab; Remodelação do músculo esquelético; Metabolismo.

resumo

Nas últimas décadas tem-se verificado um aumento significativo na taxa de sobrevivência em doentes com cancro, principalmente devido ao uso de novas modalidades de tratamento, envolvendo a quimioterapia e a imunoterapia. No entanto, a utilização de muitos destes tratamentos, como os que envolvem a administração de doxorrubicina e trastuzumab, é limitada pela sua toxicidade. Com o objetivo de melhor compreender a toxicidade associada ao tratamento com doxorrubicina e trastuzumab, na primeira parte desta dissertação procedeu-se a uma revisão dos mecanismos moleculares regulados por estes tratamentos nas diferentes células que constituem o coração. Ênfase é dado ao envolvimento da sinalização mediada por ROS e HER2 na cardiotoxicidade induzida por esta abordagem terapêutica, mas outras vias moleculares são criticamente analisadas.

Para além do impacto negativo que exerce na função cardíaca, o tratamento com doxorrubicina também pode comprometer a função do músculo esquelético, afetando a qualidade de vida dos pacientes oncológicos. Com o objetivo de compreender melhor a toxicidade induzida pela doxorrubicina no músculo esquelético, procedeu-se a um estudo experimental com ratinhos macho adultos expostos a tratamento com doxorrubicina durante 3 semanas (dose cumulativa de 9mg/Kg ou 18mg/Kg). No final do protocolo animal recolheram-se os músculos *soleus* e *gastrocnemius*. Uma vez que o músculo *soleus* foi o que evidenciou sinais macroscópicos de atrofia, procedeu-se à sua análise bioquímica, com particular destaque para as adaptações metabólicas e mecanismos regulatórios envolvidos. De facto, os nossos resultados revelaram um aumento significativo dos níveis das enzimas glicolíticas GAPDH e PFK1, após a administração de doxorrubicina, indicando uma maior dependência metabólica do músculo *soleus* pela glicólise para fins energéticos. Curiosamente, esta adaptação metabólica não foi acompanhada por alterações na dinâmica mitocondrial e na via ubiquitina proteassoma. Em conclusão, o nosso estudo mostra que o tratamento com doxorrubicina promove a remodelação do músculo *soleus*, principalmente a nível metabólico. No entanto, serão necessárias mais análises para melhor compreender os mecanismos reguladores subjacentes à remodelação molecular promovida pela doxorrubicina no músculo esquelético.

keywords

Cardiotoxicity; Doxorubicin; Trastuzumab; Skeletal muscle remodeling; metabolism.

abstract

In the last few decades, there has been a significant increase in the survival rate of cancer patients, mainly due to the use of ever-improving treatment modalities, such as chemotherapy and immunotherapy. However, the use of these treatments, such as the ones involving doxorubicin and trastuzumab, have been accompanied by severe toxicity, especially with serious cardiac toxicity. To better understand the toxicity induced by doxorubicin plus trastuzumab, in the first part of this thesis, it is presented a review integrating the molecular mechanisms harbored in the different cardiac cell types and regulated by these therapeutic approaches. This analysis emphasizes the involvement of ROS and HER2 signaling in the damaging effect of this combined treatment, but other pathways intervene. In addition to cardiotoxicity, doxorubicin may also impact skeletal muscle function, consequently affecting the quality of life of cancer patients. Thus, to better understand the toxicity induced by doxorubicin in skeletal muscle, adult male mice were exposed to treatment with doxorubicin for 3 weeks (cumulative dose of 9mg/Kg or 18mg/Kg). At the end of the protocol, *soleus* and *gastrocnemius* muscles were collected. Our study focused on the molecular remodeling of the *soleus* muscle since macroscopic signs of atrophy induced by doxorubicin were observed. The biochemical analysis focused on the effect of doxorubicin on *soleus* metabolic adaptations and regulatory mechanisms involved. Data revealed a significant increase in GAPDH and PFK1 levels, after doxorubicin administration, indicating a metabolic shift in favor of glycolysis for energetic purposes. This metabolic adaptation was not accompanied by changes in mitochondrial dynamics and in the regulation of ubiquitin-proteasome pathway. In conclusion, our study shows that doxorubicin treatment in mice promotes the remodeling of *soleus* muscle, mainly at the metabolic level; however, more pathways should be evaluated to better comprehend the molecular adaptations promoted by doxorubicin in skeletal muscle and their functional impact.

Table of Contents

Figure Index	iii
Table Index.....	v
Abbreviations	vii
CHAPTER I	1
General Introduction	1
1. Introduction	3
2. Aims	5
CHAPTER II	11
Review. Revisiting the signaling pathways underlying doxorubicin plus trastuzumab induced cardiotoxicity	11
1. Introduction	13
2. The molecular mechanisms modulated by doxorubicin in cardiomyocytes	14
3. The molecular mechanisms modulated by trastuzumab in cardiomyocytes	22
4. The molecular mechanisms modulated by doxorubicin and trastuzumab in cardiac progenitor cells	25
5. The molecular mechanisms modulated by doxorubicin and trastuzumab in endothelial cells	27
6. Molecular mechanisms modulated by doxorubicin and trastuzumab in fibroblasts 	30
7. Molecular mechanisms modulated by doxorubicin and trastuzumab in leukocytes 	30
8. Concluding remarks	31
CHAPTER III	50
Experimental work. Exploring the effects of doxorubicin on skeletal muscle remodeling	50
1. Introduction	52
2. Materials and Methods	53
2.1 Animals and experimental design	53
2.2 Morphological analysis of <i>soleus</i> muscle	54
2.3 <i>Soleus</i> homogenate preparation	54

2.4 Total protein quantification	54
2.5 Immunoblot analysis	55
2.6 Slot-blot assessment of carbonylated proteins	56
2.7 Spectrophotometric activity assays	56
2.7.1 ATP synthase activity	56
2.7.2 Citrate Synthase activity	57
2.8 Statistical analysis	57
3. Results	58
3.1 Effect of Dox on mice anthropometric parameters	58
3.2 Characterization of <i>soleus</i> metabolic adaptations to Dox treatment	58
4. Discussion	64
References	67
CHAPTER IV	73
Conclusion and Future Perspectives	73
Appendix	77

Figure Index

Figure 1. The signaling pathways modulated by Dox on cardiomyocytes, highlighting ROS generation, mitochondrial damage, apoptosis, disruption of calcium homeostasis, metabolic changes, auto(mito)phagy dysregulation, sex hormones regulation and activation of ET-1-mediated pathway. (Figure made with Servier Medical Art).

↑, upregulated; ↓, downregulated; AMPK, AMP-activated protein kinase; ASK1, apoptosis signal-regulating kinase 1; ATP, adenosine triphosphate; Bnip3, Bcl-2-like19kDa-interacting protein 3; Ca²⁺, calcium ion; Cyt c, cytochrome c; Dox, doxorubicin; Doxol, doxorubicinol; Dox-SQ, doxorubicin semiquinone; DR, death receptor; ER, estrogen receptor; ET-1, endothelial-1; ET-A, endothelial receptor A; FAO, fatty acid oxidation; Fe²⁺, ferrous ion; IRP-1, iron regulatory protein 1; JNK, c-Jun NH2-terminal kinase; MDR, multiple drug resistance; mPTP, mitochondrial permeability transition pore; Na⁺, sodium ion; NF-kB, nuclear factor kappa B; NRG-1, neuregulin-1; PLC, phospholipase C; ROS, reactive oxygen species; TopIIβ, topoisomerase IIβ.16

Figure 2. Trastuzumab-mediated signaling pathways in cardiomyocytes evidencing HER2, NRG-1 and ANG II mediated pathways. (Figure made with Servier Medical Art).

↑, upregulated; ↓, downregulated; Akt, protein kinase B; ANG II, angiotensin II; AT1, angiotensin II receptor type 1; ATP, adenosine triphosphate; Bad, Bcl-2 associated agonist of cell death; Cyt c, cytochrome c; Dox, doxorubicin; ER, estrogen receptor; ERK1/2, extracellular signal-regulated kinase 1/2; FAK, focal adhesion kinases; Grb2, growth factor receptor-bound protein 2; HER2, human epidermal growth factor receptor 2; HER4, human epidermal growth factor receptor 4; MEK1/2, mitogen-activated protein kinase kinase 1/2; NRG-1, neuregulin-1; P, phosphoryl; PI3K, phosphatidylinositol 3-kinase; PKC, protein kinase C; ROS, reactive oxygen species; SOS, son of sevenless; TopIIβ, topoisomerase IIβ. 24

Figure 3. The molecular pathways modulated by Dox and trastuzumab in cardiac progenitor cells (Figure made with Servier Medical Art).

↑, upregulated; ↓, downregulated; ASK1, apoptosis signal-regulating kinase 1; CDK-4, cyclin-dependent kinase 4; Dox, doxorubicin; HER2, human epidermal growth factor receptor 2; HGF, Hepatocyte growth factor; IGF-1, insulin-like growth factor 1; JNK, c-Jun NH2-terminal kinase; P, phosphoryl; ROS, reactive oxygen species; VEGF, vascular endothelial growth factor. 27

Figure 4. The molecular pathways modulated by Dox and trastuzumab in endothelial cells, leukocytes and cardiac fibroblasts, and their interplay and impact on cardiomyocytes homeostasis (Figure made with Servier Medical Art).

↑, upregulated; ↓, downregulated; ADCC, antibody-dependent cell-mediated cytotoxicity; ANG II, angiotensin II; AT1, angiotensin II receptor type 1; ATP, adenosine triphosphate; Dox, doxorubicin; Dox-SQ, doxorubicin semiquinone; ECM, extracellular matrix; eNOS, endothelial nitric oxide synthase; ET-1, endothelial-1; ET-B, endothelial receptor B; HER2, human epidermal growth factor receptor 2; HER4, human epidermal growth factor receptor 4; iNOS, inducible nitric oxide synthase; MMP1, matrix metalloproteinase-1; NF-kB, nuclear factor kappa B; NO, nitric oxide; NRG-1, neuregulin-1; O₂, molecular oxygen; O₂⁻, superoxide anion; ONOO⁻, peroxynitrite; P, phosphoryl; PKC, protein kinase C; ROS, reactive oxygen species; α-SMA, α-smooth muscle actin; TGF-β, Transforming growth factor-β. 29

Figure 5. Effects of Dox 9mg/Kg and Dox 18mg/Kg on different molecular markers of metabolism: **(A)** GAPDH content; **(B)** ATP synthase β subunit protein content; **(C)** Ratio between GAPDH and ATP synthase β subunit; **(D)** ATP synthase activity; **(E)** PFK-1 content; **(F)** ETFDH content. Representative blots are shown above the corresponding graphics for A, B, E and F – samples were loaded in the gel one per group side-by-side. The values (mean ± SD) are expressed in arbitrary units of optical density (OD) for A, B, E and F of n=4-6, and in nmol/min/mg for D of n=6. * p<0.05; ** p<0.01; ***p<0.001. 60

Figure 6. Effects of Dox 9mg/Kg and Dox 18mg/Kg on the levels of OXPHOS subunits. **(A)** Representative western blot for OXPHOS complexes subunits; **(B)** Expression levels of complex II, CII-SDHB, **(C)** complex III, CIII-UQCRC2, and **(D)** complex IV, CIV-COX II.

The values (mean ± SD) are expressed in arbitrary units of optical density (OD) of n=6. 61

Figure 7. Effects of Dox 9mg/Kg and Dox 18mg/Kg on the protein carbonylated levels; above the graph is presented a representative image of the slot-blot obtained – samples were loaded in the gel one per group side-by-side. The values (mean ± SD) are expressed in arbitrary units of optical density (OD) of n=6..... 62

Figure 8. Effects of Dox 9mg/Kg and Dox 18mg/Kg on citrate synthase activity (A) and Atg5 levels (B). The values (mean ± SD) are expressed in nmol/min/mg of n=6 for CS activity and in arbitrary units of optical density (OD) for Atg5 content of n=6. 63

Figure 9. Effects of Dox 9mg/Kg and Dox 18mg/Kg on the content of atrogen-1 (A) and MURF-1 (B) measured by western blotting; above each graph is presented a representative image of the western blots obtained – samples were loaded in the gel one per group side-by-side. The values (mean ± SD) are expressed in arbitrary units of optical density (OD) of n=6. 63

Figure S1. Representative images of hematoxylin and eosin stained *soleus* muscle sections, from CTRL (A), Dox 9 mg/Kg (B) and Dox 18 mg/Kg (C), groups. As can be seen, there are streaks in muscle fibers that appear to result from the technical procedure and not from the condition under study. 79

Table Index

Table 1. The effect of Dox treatment (9 mg/Kg and 18 mg/Kg) on body weight, *gastrocnemius* muscle mass, *soleus* muscle mass and on *gastrocnemius* mass-to-body weight and *soleus* mass-to-body weight ratios. Values are expressed as mean ± standard deviation of n=6. 58

Abbreviations

ADCC Antibody-dependent cell-mediated cytotoxicity

Akt Protein kinase B

AMPK AMP-activated protein kinase

ANG II Angiotensin II

AR Androgen receptor

ASK1 Apoptosis signal-regulating kinase 1

AT1 Angiotensin II receptor type 1

ATP Adenosine triphosphate

Bad Bcl-2 associated agonist of cell death

BC Breast cancer

Bcl-2 B-cell lymphoma-2

Bcl-xL B-cell lymphoma-long

Bcl-xS B-cell lymphoma-short

Bnip3 Bcl-2-like 19kDa-interacting protein 3

BSA Bovine serum albumin

CDK-4 Cyclin-dependent kinase 4

CPCs Cardiac progenitor cells

CS Citrate synthase

CTRL Control

CV Cardiovascular

Cyt c Cytochrome c

DISC Death inducing signaling complex

DNP 2,4-dinitrophenil

DNPH 2,4-dinitrophenylhydrazine

DTNB 5,5'-dithiobis-(2-nitrobenzoate)

Dox Doxorubicin

Doxol Doxorubicinol

Dox-SQ Doxorubicin semiquinone

DR Death receptor

ECs Endothelial cells

ECL Enhanced chemiluminescence

ECM Extracellular matrix

eNOS Endothelial nitric oxide synthase

ER Estrogen receptor

ERK1/2 Extracellular signal-regulated kinase 1/2

ET-1 Endothelial-1

ET-A Endothelial receptor A

ET-B Endothelial receptor B

ETFDH ETF dehydrogenase

FAK Focal adhesion kinases

FAO Fatty acid oxidation

GAPDH Glyceraldehyde-3-phosphate dehydrogenase

GSH Glutathione

GPx Glutathione peroxidase

Grb2 Growth factor receptor-bound protein 2

H&E Haematoxylin–eosin

HER2 Human epidermal growth factor receptor 2

HER4 Human epidermal growth factor receptor 4

HGF Hepatocyte growth factor

IGF-1 Insulin-like growth factor 1

iNOS Inducible nitric oxide synthase

IREs Iron-responsive elements

IRP-1 Iron regulatory protein 1

JNK c-Jun NH2-terminal kinase

KH₂PO₄ Potassium dihydrogen phosphate

LV Left ventricular

LVEF Left ventricular ejection fraction

MDR Multiple drug resistance

MEK1/2 Mitogen-activated protein kinase kinase 1/2

MMPs Metalloproteinases

MMP1 Matrix metalloproteinase-1

MnSOD Manganese-dependent superoxide dismutase

mPTP Mitochondrial permeability transition pore

MRP1 Multidrug resistance protein 1

mtDNA Mitochondrial DNA

nDNA Nuclear DNA

NK-κB Nuclear factor kappa B

NO Nitric oxide

NOS Nitric oxide synthases

NRG-1 Neuregulin-1

3-NT-Tyr 3-nitrotyrosine

O₂• Superoxide anion

OAA Oxaloacetate

OD Optical density

ONOO- Peroxynitrite

OXPHOS Oxidative Phosphorylation

P Phosphoryl

PFK-1 Phosphofructokinase-1

PgR Progesterone receptor

PI3K Phosphatidylinositol 3-kinase

PIP2 Phosphatidylinositol 4,5-biphosphate

PIP3 Phosphatidylinositol 3,4,5-triphosphate

PKC Protein kinase C

PLC Phospholipase C

PUFA Polyunsaturated fatty acids

Rb Retinoblastoma protein

RNS Reactive nitrogen species

ROS Reactive oxygen species

SDS Sodium dodecyl sulphate

SD Standard deviation

SLC Solute carrier

SOS Son of sevenless

TBS Tris-buffered saline

TCA Tricarboxylic acid

TFAM Mitochondrial transcription factor A

TGF- β Transforming growth factor- β

TNB 2-nitro-5-thiolbenzoate

TNFR1 TNF receptor 1

TnT Troponin T

Top II β Topoisomerase II β

UPS Ubiquitin-proteasome system

VEGFs Vascular endothelial growth factors

WB Western blot

CHAPTER I

General Introduction

1. Introduction

Cancer is the second leading cause of death worldwide (1); however, over the past few decades, the survival rate of cancer patients has significantly increased, regardless of the growth and aging of the population (2). This improvement in survival is explained by the ever-improving treatment modalities (3). New drugs have been developed, treatments have been combined in new ways, and optimal dosing and scheduling have been identified for existing treatments. There are many classes of chemotherapy drugs, often used in different combinations and strengths (4,5). Among these, anthracyclines represent a highly effective option for a wide range of tumors since their discovery in the 1970s (6). The main antitumor effect of anthracyclines appears to be the inhibition of topoisomerase II, through intercalation in DNA, thus causing both cytotoxicity and apoptotic death of tumor cells (7). Unfortunately, their potent antitumor activity has been hampered by severe tissue toxicities, especially muscular (cardiac and non-cardiac) toxicity (8). Chemotherapy-related cardiovascular (CV) complications include left ventricle ejection fraction (LVEF) dysfunction (usually asymptomatic but in some cases associated with clinical heart failure), progression of coronary artery disease, hypertension, thromboembolism, arrhythmias, among others (9). Indeed, after treatment with Dox, the most widely used anthracycline, the occurrence of congestive heart failure is approximately 4% with a dose of 500-550 mg/m² but increases to 18% with a dose of 551-600 mg/m² and 36% with a dose higher than 601 mg/m² (10). Although the toxicity induced by Dox is related to the cumulative dose, toxicity is often found in patients with low doses, which reveals that a lower dose of this drug does not prevent the toxicity induced by it (11).

The precise molecular mechanisms by which Dox induces cardiac dysfunction are still not completely elucidated (12). Despite various and interconnected intracellular signaling pathways have been described, several studies indicate reactive oxygen species (ROS) production as the major mechanism underlying Dox-induced cardiotoxicity (12,13). Excessive ROS lead to the damage of mitochondria, which in turn, produces more ROS, forming a vicious cycle (14). Given the high quantity of mitochondria present in cardiomyocytes, the heart is especially harmed by Dox (15). Nevertheless, other molecular pathways were implicated in Dox toxicity, such as neuroregulin-1 and endothelin-1 mediated ones (16,17).

The likelihood of developing Dox-induced cardiotoxicity increases when combined with other potentially cardiotoxic drugs like trastuzumab (18). Trastuzumab is a recombinant humanized monoclonal antibody, developed to treat patients with overexpression of human epidermal growth factor receptor 2 (HER2) oncogene, which happens in approximately 25% of breast cancer (BC) patients (18) and in about of 17.9% of gastric and gastroesophageal cancer patients (19). In the setting of BC, it is estimated that 1% to 4% of patients treated with trastuzumab develop overt heart failure, and nearly 10% to 23% experience LVEF reduction; however, this cardiotoxicity is often reversible (20). Several studies suggest that when trastuzumab and anthracyclines are concomitantly used, the incidence of trastuzumab-induced cardiotoxicity is significantly increased (21,22). Even so, the combination of Dox and trastuzumab is used as standard care in the treatment of patients with BC (20,23). Nevertheless, the molecular mechanisms behind the cardiotoxicity associated with this treatment combination remain elusive (24).

In addition to the cardiotoxicity associated with the use of anthracyclines, Dox treatment also contributes to the development of body wasting and fatigue in cancer patients, which negatively impacts quality-of-life and increases the risk of morbidity and mortality in these patients (25). These side-effects are associated, at least in part, to skeletal muscle wasting and seem to be dose-dependent, with higher doses of Dox promoting more muscle atrophy (26). Several studies have attempted to identify the molecular mechanisms responsible for Dox toxicity in skeletal muscle, envisioning to develop strategies to prevent or counteract such toxicity (27,28). Although the complete understanding of the mechanisms responsible for Dox-related toxicity in muscle remains vague, experimental studies suggest that mitochondrial dysfunction plays a central role (28). Dox-induced mitochondrial impairment results from a robust increase in ROS production, which seems to occur at several sites. Nevertheless, the primary site of ROS production occurs at oxidative phosphorylation (OXPHOS) complex I via the single electron reduction of Dox (26). An unstable semiquinone is generated and forms a redox cycle, donating an electron to oxygen to form the superoxide radical, that in turn enhances ROS production and mitochondrial dysfunction (29). This Dox-related increase in ROS production is associated with enhanced myofibrillar and cytosolic protein degradation, disrupting muscle contraction and causing fiber atrophy (30). Dox seems to induce an imbalance between anabolic and catabolic pathways in skeletal muscle towards the inhibition of protein synthesis and acceleration of proteolysis (31). In

addition, alterations in fibers metabolism have been demonstrated in skeletal muscle after Dox administration. Indeed, this drug has been shown to induce oxidative-to-glycolytic metabolic shift in *soleus* muscle (31,32). Metabolic changes that impair the adequate ATP production by OXPHOS and glycolysis and the accumulation of their metabolic by-products may lead to skeletal muscle fatigability (33). The mechanisms by which Dox impairs skeletal muscle functionality need to be further clarified, envisioning the development of strategies to counteract the associated morbidity.

2. Aims

The precise molecular mechanisms by which Dox and trastuzumab induce cardiac dysfunction are still not completely elucidated. To provide additional insight on this topic, an integrated and critical overview of the signaling pathways triggered by Dox and trastuzumab in cardiac cells is performed in a narrative review presented in chapter II.

To contribute to the better comprehension of Dox-induced toxicity on skeletal muscle, we performed an experimental work (chapter III) using adult male mice exposed to chronic treatment with Dox (cumulative dose of 9 mg/Kg or 18 mg/Kg). Our aim was to characterize the *soleus* muscle remodeling induced by Dox, through the biochemical analysis of the metabolic adaptations and regulatory mechanisms involved.

References

1. Nagai H, Kim YH. Cancer prevention from the perspective of global cancer burden patterns. *Journal of Thoracic Disease*. 2017, 9:448–451.
2. Miller KD, Nogueira L, Mariotto AB, Rowland JH, Yabroff KR, Alfano CM, Jemal A, Kramer JL, Siegel RL. Cancer treatment and survivorship statistics, 2019. *CA: A Cancer Journal for Clinicians*. 2019, 69:363–385.
3. Chan HK, Ismail S. Side effects of chemotherapy among cancer patients in a Malaysian general hospital: Experiences, perceptions and informational needs from clinical pharmacists. *Asian Pacific Journal of Cancer Prevention*. 2014, 15:5305–5309.
4. Raj S, Franco VI, Lipshultz SE. Anthracycline-induced cardiotoxicity: A review of pathophysiology, diagnosis, and treatment. *Current Treatment Options in Cardiovascular Medicine*. 2014, 16:1-14.
5. Gilliam LAA, St. Clair DK. Chemotherapy-induced weakness and fatigue in skeletal muscle: The role of oxidative stress. *Antioxidants and Redox Signaling*. 2011, 15:2543–2563.
6. Shee K, Kono AT, D’Anna SP, Seltzer MA, Lu X, Miller TW, Chamberlin MD. Maximizing the benefit-cost ratio of anthracyclines in metastatic breast cancer: Case report of a patient with a complete response to high-dose doxorubicin. *Case Reports in Oncology*. 2016, 9:840–846.
7. Marinello J, Delcuratolo M, Capranico G. Anthracyclines as Topoisomerase II Poisons: From Early Studies to New Perspectives. *International Journal of Molecular Sciences*. 2018, 19:1-18.
8. Cai F, Antonio M, Luis F, Lin X, Wang M, Cai LU, Cen C, Biskup E. Anthracycline - induced cardiotoxicity in the chemotherapy treatment of breast cancer : Preventive strategies and treatment (Review). *Molecular and Clinical Oncology*. 2019, 11:15–23.
9. Yeh ETH, Bickford CL. Cardiovascular complications of cancer therapy: incidence, pathogenesis, diagnosis, and management. *Journal of the American College of Cardiology*. 2009, 53:2231–2247.
10. Chatterjee K, Zhang J, Honbo N, Karliner JS. Doxorubicin cardiomyopathy. *Cardiology*. 2010, 115:155–62.

11. Sadurska E. Current Views on Anthracycline Cardiotoxicity in Childhood Cancer Survivors. *Pediatric Cardiology*. 2015, 36:1112–9.
12. Santos DS dos, Goldenberg RC dos S. Doxorubicin-Induced Cardiotoxicity: From Mechanisms to Development of Efficient Therapy. *Cardiotoxicity*. 2018, 3–24.
13. Cappetta D, De Angelis A, Sapio L, Prezioso L, Illiano M, Quaini F, Rossi F, Berrino L, Naviglio S, Urbanek K. Oxidative stress and cellular response to doxorubicin: A common factor in the complex milieu of anthracycline cardiotoxicity. *Oxidative Medicine and Cellular Longevity*. 2017, 2017:1-13.
14. Octavia Y, Tocchetti CG, Gabrielson KL, Janssens S, Crijns HJ, Moens AL. Doxorubicin-induced cardiomyopathy: From molecular mechanisms to therapeutic strategies. *Journal of Molecular and Cellular Cardiology*. 2012, 52:1213–1225.
15. Zhu H. Doxorubicin-Induced Cardiotoxicity. *Cardiotoxicity*. 2018, 48-66.
16. Suzuki T, Miyauchi T. A novel pharmacological action of ET-1 to prevent the cytotoxicity of doxorubicin in cardiomyocytes. *American Journal of Physiology - Regulatory Integrative and Comparative Physiology*. 2001, 280:1399-1406.
17. Liu FF, Stone JR, Schuldt AJT, Okoshi K, Okoshi MP, Nakayama M, Ho KKL, Manning WJ, Marchionni MA, Lorell BH, Morgan JP, Yan X. Heterozygous knockout of neuregulin-1 gene in mice exacerbates doxorubicin-induced heart failure. *American Journal Physiology. Heart and Circulatory Physiology*. 2005, 289:H660-H666.
18. Goldhar HA, Yan AT, Ko DT, Earle CC, Tomlinson GA, Trudeau ME, Krahn MD, Krzyzanowska MK, Pal RS, Brezden-Masley C, Gavura S, Lien K, Chan KKW. The Temporal Risk of Heart Failure Associated With Adjuvant Trastuzumab in Breast Cancer Patients : A Population Study. *Journal of the National Cancer Institute*. 2016, 108:1-8.
19. Lucas FAM, Cristovam SN. HER2 testing in gastric cancer: An update. *World Journal of Gastroenterology*. 2016, 22:4619–25.
20. Tarantini L, Cioffi G, Gori S, Tuccia F, Boccardi L, Bovelli D, Lestuzzi C, Maurea N, Oliva S, Russo G, Faggiano P. Trastuzumab adjuvant chemotherapy and cardiotoxicity in real-world women with breast cancer. *Journal of Cardiac Failure*. 2012, 18:113–119.
21. Zeglinski M, Ludke A, Jassal DS, Singal PK. Trastuzumab-induced cardiac

- dysfunction: A “dual-hit.” *Experimental Clinical Cardiololgy*. 2011, 16:70-74.
22. Maximiano S, Magalhães P, Guerreiro MP, Morgado M. Trastuzumab in the Treatment of Breast Cancer. *BioDrugs*. 2016, 30:75-86.
 23. Gonzalez Y, Pokrzywinski KL, Rosen ET, Mog S, Aryal B, Chehab LM, Vijay V, Moland CL, Desai VG, Dickey JS, Rao VA. Reproductive hormone levels and differential mitochondria-related oxidative gene expression as potential mechanisms for gender differences in cardiosensitivity to Doxorubicin in tumor-bearing spontaneously hypertensive rats. *Cancer Chemotherapy Pharmacology*. 2015, 76:447–459.
 24. Mohan N, Jiang J, Dokmanovic M, Wu WJ. Trastuzumab-mediated cardiotoxicity: current understanding, challenges, and frontiers. *Antibody Therapeutics*. 2018, 1:13-17.
 25. Park SS, Park HS, Jeong H, Kwak HB, No MH, Heo JW, Yoo SZ, Kim TW. Treadmill exercise ameliorates chemotherapy-induced muscle weakness and central fatigue by enhancing mitochondrial function and inhibiting apoptosis. *International Neurology Journal*. 2019, 23:S32–S39.
 26. Powers SK, Duarte JÁ, Nguyen BL, Hyatt H. Endurance Exercise Protects Skeletal Muscle Against Both Doxorubicin-induced and Inactivity-induced Muscle Wasting. *European Journal of Physiology*. 2020, 471:441–453.
 27. Julienne CM, Dumas JF, Goupille C, Pinault M, Berri C, Collin A, Tesseraud S, Couet C, Servais S. Cancer cachexia is associated with a decrease in skeletal muscle mitochondrial oxidative capacities without alteration of ATP production efficiency. *Journal of Cachexia, Sarcopenia and Muscle*. 2012, 3:265–275.
 28. Smuder AJ, Kavazis AN, Min K, Powers SK. Exercise protects against doxorubicin-induced markers of autophagy signaling in skeletal muscle. *Journal of Applied Physiology*. 2011, 111:1190–1198.
 29. Doerr V, Montalvo RN, Kwon OS, Talbert EE, Hain BA, Houstoun FE, Smuder AJ. Prevention of doxorubicin-induced autophagy attenuates oxidative stress and skeletal muscle dysfunction. *Antioxidants*. 2020, 9:1–17.
 30. Van Norren K, Helvoort AV, Argilés JM, Tuijl SV, Arts K, Gorselink M, Laviano A, Kegler D, Haagsman HP, Beek EM. Direct effects of doxorubicin on skeletal muscle contribute to fatigue. *British Journal of Cancer*. 2009, 100:311–314.

31. Fabris S, MacLean DA. Skeletal muscle an active compartment in the sequestering and metabolism of doxorubicin chemotherapy. *PLoS One*. 2015, 9:1–16.
32. Supriya R, Tam BT, Pei XM, Lai CW, Chan LW, Yung BY, Siu PMR. Doxorubicin Induces Inflammatory Modulation and Metabolic Dysregulation in Diabetic Skeletal Muscle. *Frontiers in Physiology*. 2016, 7:1–13.
33. VanderVeen BN, Fix DK, Montalvo RN, Counts BR, Smuder AJ, Murphy EA, Koh HJ, Carson JA. The regulation of skeletal muscle fatigability and mitochondrial function by chronically elevated interleukin-6. *Experimental Physiology*. 2019, 104:385–97.

CHAPTER II

Review. Revisiting the signaling pathways underlying doxorubicin plus trastuzumab induced cardiotoxicity

1. Introduction

Over the last thirty years, the survival rate of cancer patients has significantly increased due, at least in part, to the discovery of novel therapeutic options and the accessibility to earlier diagnosis (1,2). However, many of cancer survivors experience long-term side effects of treatments (3). For instance, in the set of breast cancer (BC), the most common cancer among women, cardiovascular (CV) complications are a major concern (4,5). Indeed, BC treatments and CV health have a close relationship, since the existence of previous cardiopathy can affect treatment selection, while cancer treatments can result in CV toxicities that can influence ongoing treatment and cancer mortality (5).

The exposure to traditional cytotoxic therapies, particularly anthracyclines, the setting of new antitumor agents also with harmful effects towards the heart (i.e. trastuzumab) and combined treatments (i.e. anthracyclines and trastuzumab, among other cardiotoxic combinations) increased the risk for CV events after cancer treatments (6). Anthracyclines-related CV complications include left ventricle ejection fraction (LVEF) dysfunction, which is mostly asymptomatic but can result in clinical heart failure, progression of coronary artery disease, hypertension, thromboembolism, arrhythmias, among others (7). Doxorubicin (Dox), the most widely used anthracycline, is highly active against a variety of neoplastic diseases. Nonetheless, the use of this drug is limited by the dose-dependent cardiotoxic effect (8). While acute toxicity is usually considered reversible, research suggests that anthracyclines can originate a progressive injury process that continues over the years (9), which can lead to dose-cumulative heart failure (10). The occurrence of congestive heart failure is approximately 4% with a cumulative lifelong dose of 500-550 mg Dox/m² but increases to 18% with a cumulative dose of 551-600 mg/m² and 36% with a dose higher than 601 mg/m² (11). It should be noted that the recommended lifetime cumulative dose for treatment with Dox should not exceed 550 mg/m² (12); however, patients who receive cumulative doses of 400 mg Dox/m² also exhibit cardiotoxicity (13), revealing that cumulative doses below the recommended limit also promote toxicity.

Regardless the amount of studies referring to classic chemotherapeutics-induced cardiotoxicity, the emergence of cancer targeted therapies led to the believe that some of the adverse effects of chemotherapy, like cardiotoxicity would decrease (14). Surprisingly, cardiotoxicity was more severe and frequent when newer targeted drugs like trastuzumab were applied clinically. Trastuzumab is a recombinant humanized monoclonal antibody that

was developed to treat patients with overexpression of human epidermal growth factor receptor 2 (HER2) oncogene. HER2 is a tyrosine kinase receptor that belongs to the superfamily of epidermal growth factor receptors (15). Four isoforms have been documented in humans (HER1-HER4). Each receptor consists of a single transmembrane ligand-activated tyrosine kinase and a carboxyl-terminal regulatory domain. HER2 is the only receptor of the ErbB family, also known as the EGF receptor family, that has no high-affinity ligand known; however, it is the most important receptor, because it plays a key role in cell survival and dimerizes with the other receptor isoforms (16). HER2 overexpression happens in approximately 25% of BC patients (17–20) and in 10-25% of gastric cancers (21). These patients experience more aggressive tumors and have a lower survival rate (20,22). The trastuzumab is a clinical option on those situations. The cardiotoxicity of trastuzumab varies according to the available clinical studies, but a classical report done in the clinical practice showed a higher incidence of cardiotoxicity than the initial clinical studies have demonstrated (23). Indeed, it was observed that 0.6 to 3.8% of patients treated with trastuzumab develop chronic heart failure, and nearly 4.1 to 30.1% experience significant LVEF reduction; however, this cardiotoxicity is often reversible (24). Nevertheless, several studies suggest that when trastuzumab and anthracyclines are concomitantly used, the incidence of trastuzumab-induced cardiotoxicity synergically increases (20,25). Nevertheless, the combination of Dox and trastuzumab is used as standard care in the treatment of HER2- positive BC patients (23) and the molecular mechanisms behind the cardiotoxicity associated with this treatment combination remain elusive (20). The current paper overviews, in an integrated perspective, the signaling pathways harbored in cardiomyocytes and in other cardiac cells that are modulated by Dox and trastuzumab and that impact the clinical outset of the treated patients.

2. The molecular mechanisms modulated by doxorubicin in cardiomyocytes

Dox enters cancer cells through passive diffusion, mediated by transporters or by endocytosis. Dox may establish electrostatic and hydrophobic interactions with cell membranes, enabling Dox to enter cells by passive diffusion (26,27), but Dox uptake may also be mediated by solute carrier (SLC) transporters, including SLC22A16 (28). In the nucleus, Dox intercalates into the DNA and inhibits topoisomerase II α (Top II α) through the formation of Top II-Dox-DNA ternary complex (also called the cleavage complex) (29),

hindering the proliferation of cancer cells and leading to their death (30). This mechanism is key for its anticancer properties. Nonetheless, while Dox can enter into cardiomyocytes through the same transport mechanisms, mentioned before (31,32) (Figure 1), Top II α is mainly expressed in proliferating cells, but Top II β is expressed in post mitotic cells, such as adult cardiomyocytes (33). Indeed, in cardiac cells, DNA Top II β is highly expressed, not only in the nucleus but also in the mitochondria (34). Dox conjugates with Top II β and DNA (34,35) and induces topological changes in this biomolecule, the accumulation of protein-DNA adducts, double strand breaks of nDNA or mtDNA, activating DNA damage response and apoptosis (13,30) (Figure 1). Dox can rapidly intercalate into mtDNA, inhibiting mtDNA synthesis and causing mtDNA depletion. Indeed, mtDNA represents an important cellular target of Dox, which possible contributes to the mitochondrial and, consequently, to the cardiac toxicity associated with Dox use (36). Dox modulates other molecular mechanisms in cardiomyocytes beyond Top II β inhibition. In fact, the pathophysiology of Dox-related cardiotoxicity is recognized to be a multistep process that involves the cross-talk between several signaling pathways and between different cell types (37).

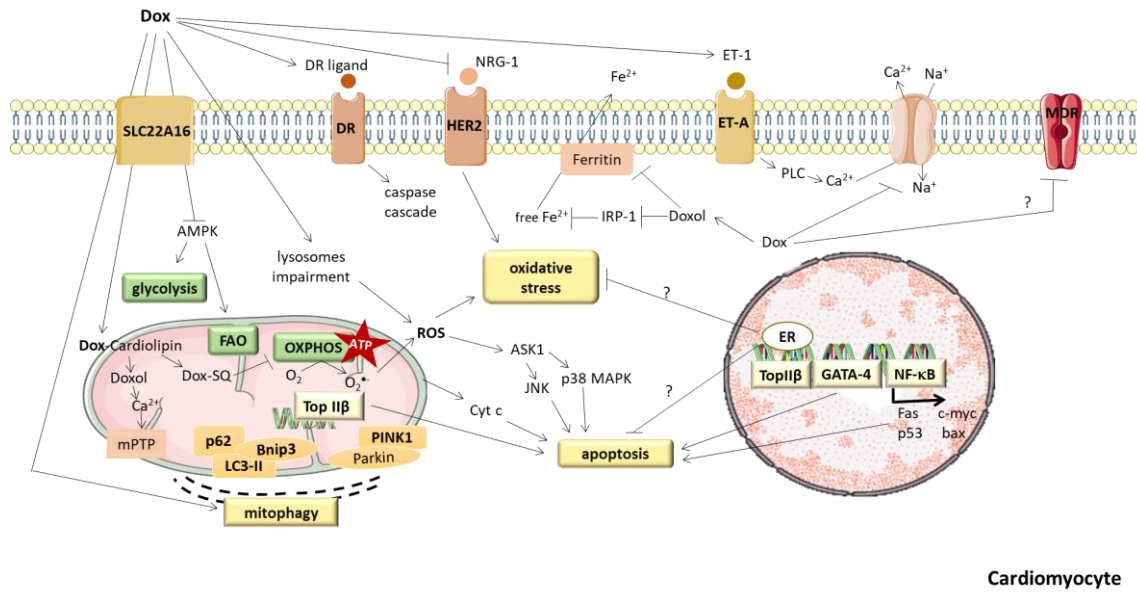


Figure 1. The signaling pathways modulated by Dox on cardiomyocytes, highlighting ROS generation, mitochondrial damage, apoptosis, disruption of calcium homeostasis, metabolic changes, auto(mito)phagy dysregulation, sex hormones regulation and activation of ET-1-mediated pathway. (Figure made with Servier Medical Art).

↑, upregulated; ↓, downregulated; AMPK, AMP-activated protein kinase; ASK1, apoptosis signal-regulating kinase 1; ATP, adenosine triphosphate; Bnip3, Bcl-2-like19kDa-interacting protein 3; Ca²⁺, calcium ion; Cyt c, cytochrome c; Dox, doxorubicin; Doxol, doxorubicinol; Dox-SQ, doxorubicin semiquinone; DR, death receptor; ER, estrogen receptor; ET-1, endothelial-1; ET-A, endothelial receptor A; FAO, fatty acid oxidation; Fe²⁺, ferrous ion; IRP-1, iron regulatory protein 1; JNK, c-Jun NH2-terminal kinase; MDR, multiple drug resistance; mPTP, mitochondrial permeability transition pore; Na⁺, sodium ion; NF-κB, nuclear factor kappa B; NRG-1, neuregulin-1; PLC, phospholipase C; ROS, reactive oxygen species; TopIIβ, topoisomerase IIβ.

2.1. Oxidative stress: the “traditional” trigger of Dox cardiotoxicity

Oxidative stress has been considered for several decades and, therefore, was the most described molecular process associated to the complex pathophysiology of Dox-induced cardiotoxicity (38). It was believed that reactive oxygen species (ROS) and reactive nitrogen species (RNS) produced by the redox cycle of Dox to its semi-quinone radical within the cardiomyocytes (39) were not effectively removed/neutralized due to low levels of cardiac antioxidant enzymes, such as glutathione peroxidase (GPx), catalase, and superoxide dismutase (SOD) (37). In fact, the heart has low levels of antioxidant systems but high oxygen consumption rates, with high basal formation of superoxide anion radical. Therefore,

cardiomyocytes are particularly prone to oxidative damage (40) (Figure 1). ROS are formed by electron exchange between the Dox quinone moiety and oxygen, and through the formation of complexes with iron (41). In physiological conditions, iron free levels are usually low and are tightly controlled; however, Dox interferes with the activity of proteins that transport and bind intracellular iron (42). Dox can interact with iron-responsive elements (IREs) of the ferritin heavy and light chains. Ferritin operates as an iron transporter, decreasing free iron within the cell. The consequent disruption of this protein expression caused by Dox eventually increases free iron (43). Next, Dox can directly bind to iron and, in the presence of oxygen, it can cycle between the Fe(II) and Fe(III) state. The reactions involved are accompanied by the formation of ROS (44), which ultimately can lead to cell death (Figure 1).

Moreover, doxorubicinol (Doxol), a Dox metabolite formed through the reduction of Dox side chain C-13 carbonyl group by NADPH-dependent aldo/ketoses or carbonyl reductases (41), seems to be more toxic to cardiac cells than Dox when formed intracellularly (45), in opposition to the observed in tumor cells (46). This metabolite, Doxol, removes iron from the catalytic Fe-S cluster of the cytoplasmic iron regulatory protein 1 (IRP-1) (47). The reduction of IRP-1 causes an increase in free iron, which might lead to ROS production, mostly through Fenton reaction (48).

One of the consequences of increased ROS generation, and the subsequent depletion of cellular glutathione (GSH), is the downregulation of multidrug resistance (MDR) transmembrane drug efflux-transporters (49). In cardiomyocytes, these transporters may protect from Dox toxicity (50), as multidrug resistance protein 1 (MRP1), a member of the subfamily C of ABC transporters, mediates the ATP-dependent efflux of a wide range of chemotherapeutic drugs, such as Dox (50). The downregulation of MRP1 was related with the rise of Dox-induced cardiotoxicity MRP1/Abcc1 null mice (50).

Oxidative stress has been considered the major trigger of Dox cardiotoxicity; however, it is uncertain if it is a cause or a consequence of Dox-induced cell damage. Moreover, prevention strategies relied on antioxidants are far from success.

2.2. Neuregulin-1 and endothelin-1 signaling pathways

The growth factor neuregulin-1 (NRG-1) and its EGFR family of tyrosine kinase, also known as ErbB or HER, might also be inhibited by Dox. NRG-1/HER2 and HER4 signaling

is critical for cardiac development (51) and for maintaining the myocardial architecture during adulthood (52). The activation of HER2 and the subsequent activation of downstream signaling may be an early survival response to Dox injury (53,54) (Figure 1). HER2 activation occurs before any evidence of functional systolic deficits caused by the anthracycline and seems to involve post-transcriptional mechanisms since no changes in HER2 mRNA were observed (54). HER2 receptor and the downstream Akt, p70S6K, and ERK-1/2 pathways were implicated in the polymerization of actin and in the synthesis of myofibrillar proteins in cardiomyocytes (55). HER2 was also involved in the regulation of antioxidant systems such as GPx and catalase, protecting cardiomyocytes from ROS-related injury (56). Moreover, mice with heterozygous knockout of the neuroregulin-1 gene and treated with Dox evidenced higher impairment of LVEF function and decreased survival compared to wild-type mice treated with this drug (53).

Dox also induces the overexpression of endothelin-1 (ET-1) (57), a potent vasoconstrictor peptide produced by the endothelium (58) and also by cardiomyocytes (59). This peptide was reported to have a positive inotropic effect on the myocardium, through the activation of phospholipase C (60) and to induce hypertrophy of cardiomyocytes (61). By increasing the release of Ca²⁺ from the sarcoplasmic reticulum through IP3 signaling, ET-1 stimulates contraction. Calcium load in cardiomyocytes also predisposes to cardiomyocytes apoptosis and cardiac dysfunction (62). Mice pretreated with an endothelin receptor antagonist attenuated Dox-induced cardiotoxicity (63).

Taken together, NRG1 seems to be effective in attenuating Dox-induced cardiac damage, whereas ET-1 potentiates it. Thus, ET-1 inhibition may present therapeutic benefits for patients treated with Dox.

2.3. Mitochondria-dependent signaling pathways

Mitochondrion has been recognized as the main organelle damaged in the heart by Dox (42). This organelle comprises up to 35% of total cardiomyocyte volume, making this cell type particularly sensitive to Dox and its metabolites (64). Indeed, aglycone metabolites of Dox were reported to have greater effects on mitochondria than the parent drug (65). One of their central molecular targets is cardiolipin (CL), a phospholipid specific of the inner mitochondrial membrane involved in the stabilization of oxidative phosphorylation (OXPHOS) complexes (66). CL is required for the structural integrity and full activity of

OXPPOS complexes (67). Being cationic, Dox can bind with high affinity to CL, an anionic molecule, forming a nearly irreversible complex with negative impact in the fluidity and functionality of mitochondrial membranes (42). Thus, Dox accumulates in mitochondria where the redox cycling of quinones will be prominent and OXPPOS complexes become uncoupled (37), resulting in decreased production of adenosine triphosphate (ATP) (68). Furthermore, the inhibition of OXPPOS complexes I and II results in increased ROS generation. The quinone moiety in Dox chemical structure is reduced by complex I into a reactive semiquinone free radical, which, in turn, when reacts with oxygen, leads to the generation of the superoxide radical anion (69), as stated before. The ROS generated either by direct cycling and by OXPPOS complexes uncoupling, disrupts intracellular and mitochondrial Ca^{2+} homeostasis, impairing normal beat-to-beat contractile activity (69). Furthermore, the increase in Ca^{2+} intracellular concentrations seems to be favored by Doxol metabolite, which inhibits the sodium/calcium exchanger channel and sodium/potassium pump at the sarcolemma (41), further impairing mitochondrial Ca^{2+} homeostasis. Mitochondrial Ca^{2+} overload prompts mitochondrial permeability transition pore (mPTP), leading to the dissipation of transmembrane potential and to increased permeability of the outer membrane (70). These disturbances might lead to ultrastructural pathologic changes, such as mitochondrial swelling and myelin figures inside the mitochondria (42).

The loss of mitochondrial membrane potential and the rupture of mitochondrial outer membrane after Dox treatment can lead to the release of cytochrome c. In the cytosol, cytochrome c activates apoptosis (71). Dox-induced apoptosis of cardiomyocytes might also occur through other mechanisms. One of them is also mediated by ROS (42), a triggering player that activates apoptosis-signal regulating kinase-1 (ASK1) and the downstream c-Jun NH2-terminal kinase (JNK), and p38 MAPK pathways (72). ROS also activates the transcription factor NF- κ B, which upregulates apoptotic genes, including Fas, c-Myc and p53 (73). The activation of p53 by superoxide radical anion and hydrogen peroxide leads to the downregulation of GATA-4 transcription factor (74) and to the overexpression of Bax genes, prompting the mitochondrial pathway of apoptosis that culminates in caspases activation (75). There are experimental evidences that support the activation of caspase-3 following Dox treatment, in both rat primary cultured cardiomyocytes and rat hearts (76). Dox-mediated apoptosis might also involve the upregulation of death receptors (DRs) (42), including the TNF receptor 1 (TNFR1), Fas, DR4 and DR5 (30). Activation of DRs

stimulates the assembly of a death-inducing signaling complex (DISC) that activates a caspase cascade and ensues the cleavage of cellular proteins, ultimately leading to the apoptosis of target cells (30) (Figure 1).

The decrease in ATP levels that follows DOX-induced mitochondria impairment leads to an increase of AMP/ATP ratio with the consequent activation of AMP-activated protein kinase (AMPK). This serine/threonine kinase senses energy status and activates metabolic pathways, such as fatty acid oxidation, to maintain energy homeostasis and protect the myocardium from apoptosis (77). However, AMPK seems to be repressed by Dox, even after acute exposure to low drug doses (78). Thus, Dox-induced inhibition of AMPK exacerbates cardiac energetic stress (79). Given the role of AMPK in the regulation of glucose and fatty acid metabolism (77), the impaired utilization of these energetic substrates is likely in Dox-treated hearts (Figure 1). Indeed, the gene expression of proteins involved in glucose and fatty acid oxidation was reported to be downregulated in rats treated with Dox (80). The inhibition of these pathways may also contribute to the activation of Akt-mTOR (81), autophagy (82) and cell death pathways (9).

Therefore, Dox has been considered a major mitochondrion toxin whether by disrupting their function and homeostasis as by unleashing several death pathways that ultimately involve this organelle.

2.4. Auto(mito)phagy dysregulation

Autophagy may also be triggered by Dox. This process comprises several steps that leads to the formation of the phagophore, which engulf the cargo, forming the autophagosome. Then, lysosomes fuse with the autophagosome and the lysosomal enzymes degrades the cargo (83,84). Dox-induced formation of autophagosomes was reported in cardiac cells, both in *in vitro* and *in vivo* (85,86). Upregulation of autophagy was associated to Dox-induced cardiotoxicity (87); however, autophagy function is dysregulated by it (88). Several studies suggest that Dox leads to an overactivation of autophagy initiation but prevents autophagy completion due to deleterious effects on lysosomes (89–91). The resulting accumulation of lysosomes' undegraded cargo promotes ROS overproduction in cells, contributing to their death (83).

The clearance of damaged mitochondria by selective autophagy (mitophagy) is also activated by Dox. Two major pathways have been described in cardiomyocytes exposed to

Dox: Parkin/PTEN-induced kinase 1 (PINK1)-mediated mitophagy and Bcl-2-like 19kDa-interacting protein 3 (Bnip3)-mediated mitophagy (92,93). PINK1 accumulates on the outer membrane of mitochondria when they lose membrane potential. Then, the E3 ubiquitin ligase parkin is recruited and once activated, elicits the ubiquitination of outer mitochondrial membrane proteins that interacts with protein p62. LC3-II may interact with p62 leading to autophagosome engulfment of mitochondria (94,95). The expression of both PINK1 and parkin was reported to be increased in response to Dox, and parkin translocation to mitochondria was verified (92). Nevertheless, a biphasic response of Parkin/PINK was verified in mice hearts following Dox administration, being characterized by low levels five days after treatment and higher levels two weeks after (96), possibly due to a putative adaptive situation. On the other hand, Bnip3-mediated mitophagy involves the translocation of Bnip3 to mitochondria and the consequent promotion of permeability transition and depolarization, functioning more upstream. Bnip3 can also recognize LC3 and trigger mitophagy. Indeed, Dox-induced mitochondrial perturbations and cell death of ventricular myocytes have been associated with Bnip3 related mechanisms (97) (Figure 1). Thus, mitophagy plays a crucial role in cardiomyocyte survival under Dox-induced stress, but beyond a certain threshold it can promote cell death (98).

2.5. Sex hormones interfere with Dox toxicity

Cardiac cells express progesterone (PgR), estrogen (ER α , ER β , and GPER) and androgen (AR) receptors that are functionally responsive to sex hormones (99) and Dox cardiotoxicity may also be modulated by these hormones. Indeed, 17 β -estradiol was reported to suppress Dox-induced oxidative damage in human cardiac cell lines (100) and in animal models (8). Dox-treated spontaneously hypertensive rats with SST-2 breast tumor showed little to no estrogen or testosterone, which was associated with higher cardiotoxicity assessed by cardiac lesion score and circulating troponin T (40). Estrogen was also reported to prevent cardiomyocyte apoptosis, relieve left ventricular hypertrophy and protect against the development of cardiac fibrosis in women (101). These protective effects of estrogen may be related to its antioxidant effect in preventing fatty acid and cholesterol peroxidation and in maintaining the levels of GPx, catalase, and SOD (102). Estrogen also seems to prevent Dox-induced cardiac metabolic stress. Indeed, Dox was shown to deregulate the cardiac energetic status in male rats, whereas energy metabolism was preserved in females under the

same therapeutic protocol (80). These data support the protective role of estrogens against Dox cardiotoxicity, possibly explaining the higher risk of postmenopausal BC patients for heart failure (103).

3. The molecular mechanisms modulated by trastuzumab in cardiomyocytes

Trastuzumab is a humanized monoclonal antibody that targets the extracellular domain of HER2, also referred to as ErbB2 (104). This first-generation targeted therapy drug when combined with chemotherapy drugs reduces the risk of HER2-positive BC and gastric cancer recurrence and death compared to chemotherapy drugs alone (21,105). In fact, it was a breakthrough in anticancer-targeted therapy. Trastuzumab binds selectively to subdomain IV of the extracellular HER2 domain, triggering its tumor-suppressive actions through multiple mechanisms. These include the activation of antibody-dependent cell-mediated cytotoxicity (ADCC), inhibition of HER2 extracellular domain cleavage, disruption of HER2 receptor homodimerization and heterodimerization, and downregulation of angiogenesis and DNA repair pathways (106). Trastuzumab has been shown to block the proteolytic cleavage of the extracellular domain of HER2, which may ultimately reduce the expression of HER2 (107). When trastuzumab was placed in the market, it was considered a selective therapy to the HER2-positive cancer, therefore no significant side effects were expected; but surprisingly adult cardiomyocytes also express HER2, and were found to be a target for trastuzumab (108). Indeed, several pathways downstream HER2 have been implicated in the cardiotoxicity induced by trastuzumab and in the clinical cardiotoxicity onset.

3.1. Downregulation of HER2 signaling and cardiotoxicity

One of the most studied pathways modulated by this drug in cardiac cells involves NRG-1 (109). NRG-1 binds to and activates HER4, which is then prepared for binding to HER2 (20). HER2/HER4 heterodimerization results in tyrosine kinase activation (16). This leads to the activation of different signaling pathways, such as the Ras/Raf/MEK/ERK1/2 pathway. The activation of these pathways involves the recruitment of son of sevenless (SOS) through intracellular Grb2 domains, ultimately catalyzing the conversion of inactive Ras-guanosine diphosphate to the active Ras-guanosine triphosphate complex, activating Raf complex. Then, MEK1/2 is phosphorylated and activated, and subsequently catalyzes

the phosphorylation of ERK1/2 (110). This enzyme translocates from the cytoplasm to the nucleus where it activates downstream transcription factors, including c-Myc, and stimulates cell survival by inhibiting apoptosis (111). By preventing the activation of this pathway, trastuzumab may promote cardiac cell apoptosis (Figure 2).

The PI3K/Akt pathway can also be activated by NRG-1 (112). Following the activation of HER2/HER4 receptor, the PI3K protein suffers phosphorylation and then phosphorylates lipids in the plasma membrane, forming the second messenger, phosphatidylinositol-3,4,5-triphosphate (PIP3). Akt is recruited into the membrane interacting with PIP3 so that it can be phosphorylated (113). Akt may phosphorylate Bad, a member of the Bcl-2 family, releasing it from the complex previously formed with Bcl-2 and Bcl-xL. These anti-apoptotic proteins inhibit cytochrome c release from mitochondria, preventing the activation of the intrinsic mitochondrial apoptosis pathway (114). On the other hand, trastuzumab in the heart downregulates Bcl-xL and upregulates Bcl-xS, a pro-apoptotic protein. This shift in the ratio between anti- and pro-apoptotic proteins towards pro-apoptotic proteins is therefore correlated with mitochondrial dysfunction leading to cardiomyocytes death (107,110). Indeed, the mitochondrial dysfunction induced by this antibody seems to be an early event given by the ultrastructural evidence of cristae disorganization observed in the cardiac muscle of rabbits (115) (Figure 2).

There is a third pathway by which trastuzumab interferes with NRG-1 cardiac signaling and it involves the focal adhesion kinases (FAKs). Once activated, FAK forms a complex with Src family kinases initiating multiple intracellular signaling pathways (20). Indeed, FAK has been shown to interplay with a variety of signaling mediators, such as PI3K and ERK, which can induce cell survival pathways (116). By inhibiting HER2 ability to dimerize and, consequently, cell survival through Ras/Raf/MEK/ERK1/2, PI3K/Akt and FAK-dependent pathways, trastuzumab makes cardiomyocytes unable to handle with additional stresses (117), as the one that happens with Dox treatment.

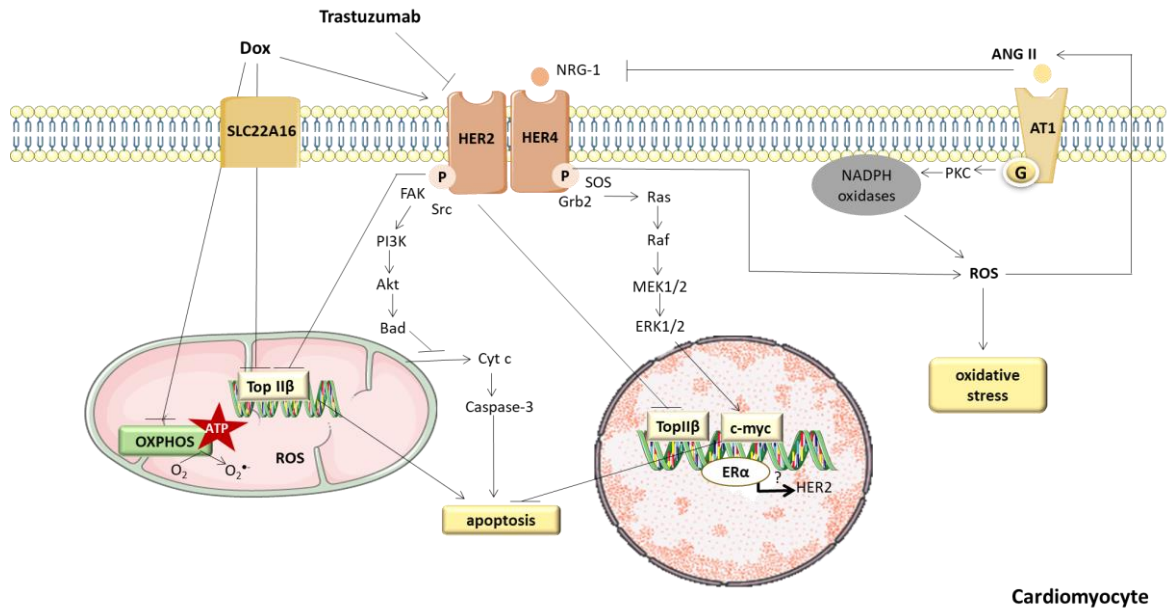


Figure 2. Trastuzumab-mediated signaling pathways in cardiomyocytes evidencing HER2, NRG-1 and ANG II mediated pathways. (Figure made with Servier Medical Art).

↑, upregulated; ↓, downregulated; Akt, protein kinase B; ANG II, angiotensin II; AT1, angiotensin II receptor type 1; ATP, adenosine triphosphate; Bad, Bcl-2 associated agonist of cell death; Cyt c, cytochrome c; Dox, doxorubicin; ER, estrogen receptor; ERK1/2, extracellular signal-regulated kinase 1/2; FAK, focal adhesion kinases; Grb2, growth factor receptor-bound protein 2; HER2, human epidermal growth factor receptor 2; HER4, human epidermal growth factor receptor 4; MEK1/2, mitogen-activated protein kinase kinase 1/2; NRG-1, neuregulin-1; P, phosphoryl; PI3K, phosphatidylinositol 3-kinase; PKC, protein kinase C; ROS, reactive oxygen species; SOS, son of sevenless; TopIIβ, topoisomerase IIβ.

3.2. Trastuzumab intensifies doxorubicin signaling in cardiomyocytes

HER2 blockade might promote ROS-mediated cardiomyocyte death (118). This is particularly worrying when trastuzumab is used in combination with Dox (107), namely when the use of Dox occurs as a primary treatment, since it damages cardiac cells through ROS-dependent pathways. Dox usage and the subsequent treatment with trastuzumab potentiates oxidative stress because it blocks NRG-1/HER2 signaling, enhancing the myocardial damage (119). Moreover, human cardiomyocytes exposed to Dox showed increased HER2 protein levels with the consequent activation of the downstream signaling pathway, possible in an adaptive response to allow survival under stress conditions (20,120), but trastuzumab blunts that response. The administration of trastuzumab followed by doxorubicin was shown to be more toxic to the heart in rats based on electron microscopy

findings, and pathological changes in mitochondria seem to explain the cardiotoxicity of this treatment combination (121).

Furthermore, HER2 seems to be upregulated by ER α , which suggests that trastuzumab-induced cardiotoxicity is modulated by female sex hormones (122), similarly to the reported for Dox (Figure 2).

Angiotensin II (ANG II) is an inhibitor of NRG-1 that prevents its binding to other ErbB receptors, being its levels also modulated by trastuzumab. ANG II interaction with NRG-1 leads to even more inhibition of NRG-1/HER2 signaling pathway (20). ANG II also negatively influences the heart by activating NAPDH oxidases in several cell populations, including cardiomyocytes. ANGII binds to AT1 receptor, a G-protein coupled receptor that acts through protein kinase C (PKC) and activates NAPDH oxidases. The consequent increase of ROS generation, as a result of that activation, causes oxidative stress and apoptosis (123) (Figure 2).

Finally, DNA Top II β , a major target for Dox-inflicted cardiotoxicity, is also downregulated by trastuzumab. An *in vitro* study showed that trastuzumab either alone or in combination with Dox negatively impacts Top II β (120). The downregulation of this topoisomerase was reported to be significantly enhanced when cardiomyocytes were treated with the combination of Dox and trastuzumab, either sequentially, being Dox first, or concurrently (120).

Taken together, the damage of cardiomyocytes inflicted by Dox plus trastuzumab is due to a combination of “on-” and “off-target“ effects, involving NRG1/HER2 and ANGII/AT1 signaling and TopII β downregulation.

4. The molecular mechanisms modulated by doxorubicin and trastuzumab in cardiac progenitor cells

Most of the research on the molecular mechanisms underlying the cardiotoxicity induced by anticancer drugs has focused on cardiomyocytes; however, other heart cells may also be involved (124). Cardiac progenitor cells (CPCs) are one of the best characterized populations of the endogenous pool of cells known to contribute to cardiac repair (125). Some data showed that Dox targets CPCs, negatively affecting its biological function (126,127). Dox induces apoptosis, telomere shortening and senescence of CPCs, reducing the pool of

available CPCs for the restoration of the functional performance of the heart. Thus, Dox treatment impairs the capacity of the heart to deal with continuous stress (128).

Dox has negative effects on the levels of phosphorylated SIRT1, leading to increased levels of acetylated p53 and the consequent activation of pro-apoptotic genes (127). CPCs apoptosis may be associated to ROS generation, to which CPCs are particularly sensitive (128). Dox also increases the expression of p16^{INK4A} in CPCs, causing cell cycle arrest in the G1 phase and senescence. Data suggest that p53 induces the senescence response and p16^{INK4A} maintains this state. (128). Furthermore, CPCs exposed to Dox showed a reduction in the levels of cyclin D1 and cyclin-dependent kinase 4 (CDK-4) (129). These proteins work together to phosphorylate the retinoblastoma protein (Rb) into phospho-Rb^{Ser798}, allowing the cell cycle progression (130).

Treatment with Dox was also reported to reduce the expression of insulin-like growth factor 1 (IGF-1) and hepatocyte growth factor (HGF) receptors in CPC (128,131,132) (Figure 3). IGF-1 receptor has proliferative and anti-apoptotic effects in CPCs, while HGF receptor supports cell migration in the direction of injury areas, which is thought to be essential for tissue repair in response to damage (132,133). In addition, Dox-induced depletion of CPCs pool may be associated with autophagy signaling, which seems to be triggered by abnormal cytosolic Ca²⁺ handling. Lower expression levels of autophagosome formation markers (LC3-I and LC3-II) was observed in c-kit^{POS} CPCs isolated from infant human heart tissue and exposed to Dox (134).

Treatment with trastuzumab has been reported to negatively affect the biological functions of CPCs (135). Indeed, the cardiogenic differentiation and the capability to form microvascular networks by CPCs were reported to be impaired after treatment with trastuzumab (136). Even though cardiomyogenesis and angiogenesis inhibition was reported after trastuzumab treatment (136), the molecular mechanisms harbored in CPCs and modulated by trastuzumab are yet unclear. Experimental evidence is also missing regarding the effect of the combined use of doxorubicin and trastuzumab on CPCs.

Cardiac progenitor cell

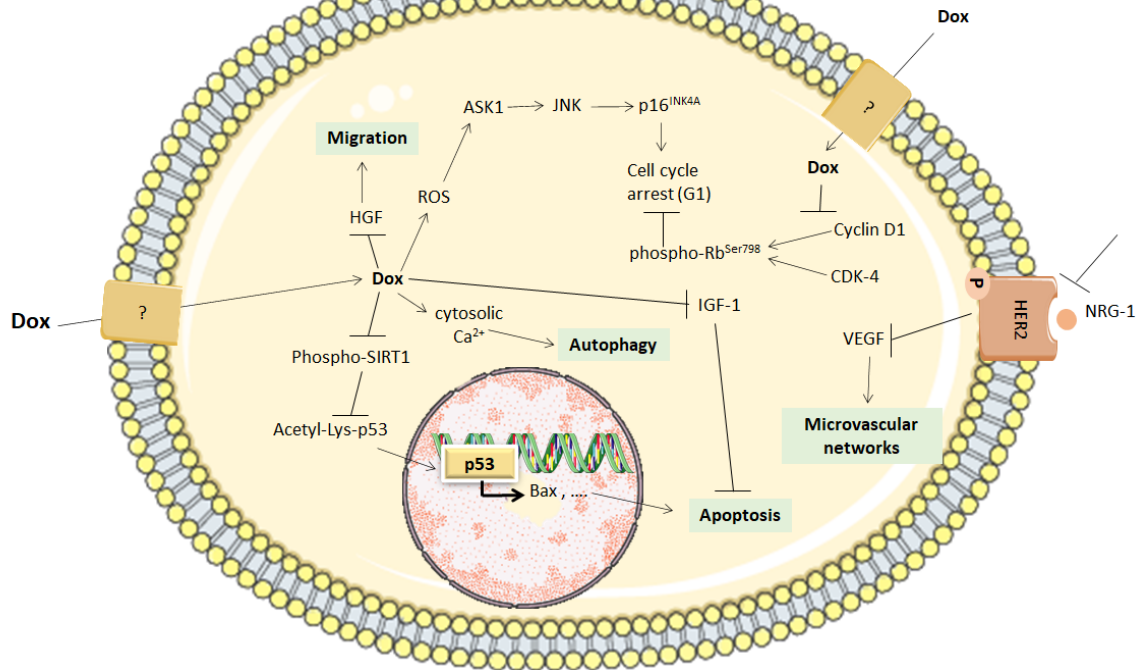


Figure 3. The molecular pathways modulated by Dox and trastuzumab in cardiac progenitor cells (Figure made with Servier Medical Art).

↑, upregulated; ↓, downregulated; ASK1, apoptosis signal-regulating kinase 1; CDK-4, cyclin-dependent kinase 4; Dox, doxorubicin; HER2, human epidermal growth factor receptor 2; HGF, Hepatocyte growth factor; IGF, insulin-like growth factor 1; JNK, c-Jun NH2-terminal kinase; P, phosphoryl; ROS, reactive oxygen species; VEGF, vascular endothelial growth factor.

5. The molecular mechanisms modulated by doxorubicin and trastuzumab in endothelial cells

Endothelial cells (ECs) represent the majority of non-cardiomyocytes heart cells (137) and may be directly affected by Dox and trastuzumab. For instance, Dox can enter ECs through SLC22A1, which is highly express in these cells (138). There, Dox may interfere with the endothelial nitric oxide synthase (eNOS) (42), whose activity is normally regulated by cytosolic Ca^{2+} levels through the calmodulin subunit of the enzymatic complex (oxygenase domain) (139). The reductase domain of eNOS can bind to Dox and reduce it to the semiquinone radical with the consequent enhancement of superoxide anion radical formation and decreased nitric oxide (\bullet NO) production (140). Hence, Dox converts eNOS from a \bullet NO to a superoxide generator (70). The consumption of NADPH becomes uncoupled from \bullet NO production, which leads to reduce \bullet NO available levels and increases

superoxide anion radical levels. Despite lower •NO levels, increased nitrosative stress was reported following Dox treatment (141). Peroxynitrite (ONOO⁻) is a powerful and reactive oxidant that results from the reaction between •NO and superoxide anion radical (141). Nonetheless, the peroxynitrite formed in endothelial cells seems to involve •NO derived from iNOS activity, whose expression was reported to increase in cardiomyocytes following Dox treatment (141). Peroxynitrite can react with protein tyrosine residues, resulting in the post-translational modification 3-nitrotyrosine (3-NT-Tyr) (141,142), which may inactivate some proteins (e.g. MnSOD) and promote the gain-of-function of others (e.g. fibrinogen) (143). Peroxynitrite-dependent cytotoxic effects also rely on its ability to trigger lipid peroxidation in membranes by abstracting a hydrogen atom from polyunsaturated fatty acids (PUFA), resulting in products such as lipid hydroperoxyradicals (140). These radicals attack neighboring PUFAs, generating additional radicals, which propagate free radical reactions and the degeneration of membrane lipids, causing membrane permeability (144) and fluidity changes (142) as a result of lipid peroxidation (Figure 4).

Following Dox treatment, the expression of ET-1 increases in cardiomyocytes; however, the decreased expression of ET-1 was reported in cultured ECs treated with low concentrations of Dox (145). Thus, different regulatory mechanisms of ET-1 expression seem to be present in cardiomyocytes and in ECs. Indeed, the formation of the active ET-1 peptide is a multistep process, regulated at several steps including those of transcription, mRNA stabilization, translation, release, and the cleavage from big ET-1 (146). ET-1 acts on target tissues through two receptors, type A receptor (ET-A) and type B receptor (ET-B), which belong to the plasma membrane protein G receptor superfamily (147). ET-A receptors are abundantly present in cardiomyocytes (148), mediating the effect of ET-1 (Figure 1). ET-1 binds to the ETB receptors on the ECs membrane and induces the release of relaxing factors, such as •NO (149). Thus, the Dox-induced reduction of ET-1 in ECs leads to the decrease of •NO levels in those cells (150) (Figure 4), unlike to what has been reported in cardiomyocytes.

The association between endothelial dysfunction and trastuzumab-induced cardiotoxicity has been described (151). ECs seem to be damaged in HER2-positive BC patients treated with trastuzumab, leading to a reduction in eNOS expression and endothelial dysfunction (152). In fact, ECs from human cardiac microvasculature are known to express HER2 receptor (153). The administration of trastuzumab inhibits HER2 receptor, preventing

its dimerization with the NRG-1/HER4 complex. Subsequently, there is a reduction in eNOS expression and •NO bioavailability, predisposing the vessels to atherosclerosis (152) (Figure 4).

The inhibition of the NRG-1/HER2 pathway by trastuzumab also promotes the increased production of ROS in ECs (151), which leads to an increment in the levels of ANG II. ANG II inhibits NRG-1 activity in the coronary microvasculature and increases the levels of NADPH oxidases (152). Indeed, NADPH oxidase has been considered a causal factor of endothelial dysfunction due to its capability to generate large amounts of ROS in the endothelium (154) (Figure 4). These processes culminate in endothelial dysfunction, which is an important contributor to heart failure (151).

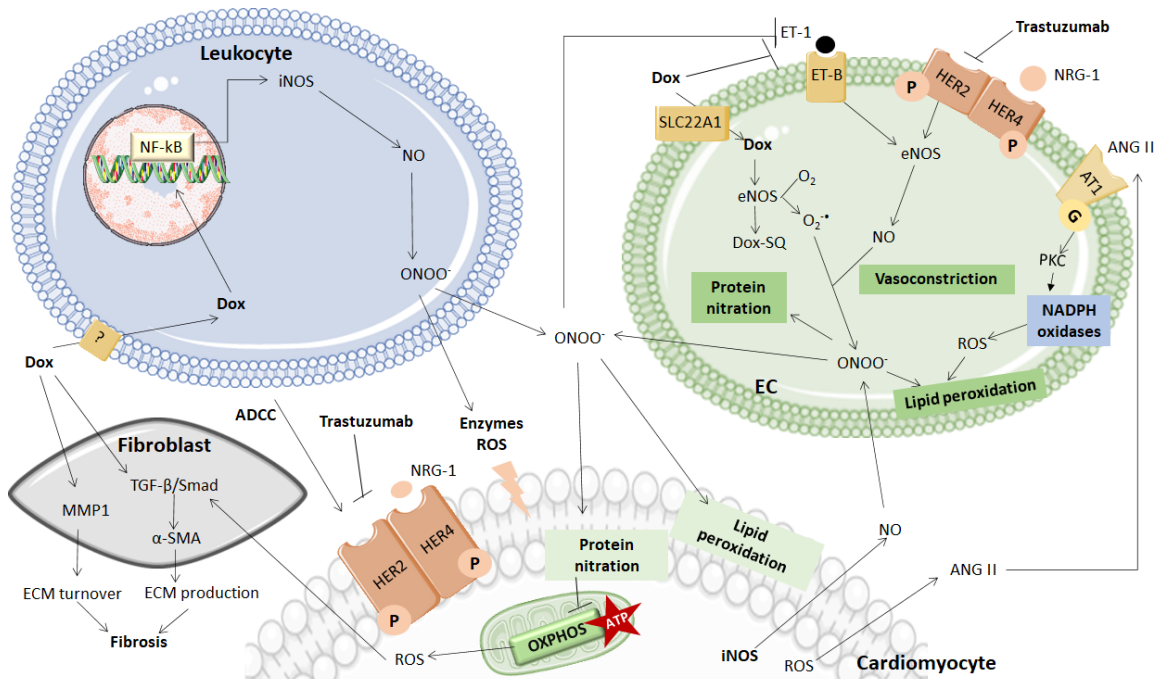


Figure 4. The molecular pathways modulated by Dox and trastuzumab in endothelial cells, leukocytes and cardiac fibroblasts, and their interplay and impact on cardiomyocytes homeostasis (Figure made with Servier Medical Art).

↑, upregulated; ↓, downregulated; ADCC, antibody-dependent cell-mediated cytotoxicity; ANG II, angiotensin II; AT1, angiotensin II receptor type 1; ATP, adenosine triphosphate; Dox, doxorubicin; Dox-SQ, doxorubicin semiquinone; ECM, extracellular matrix; eNOS, endothelial nitric oxide synthase; ET-1, endothelial-1; ET-B, endothelial receptor B; HER2, human epidermal growth factor receptor 2; HER4, human epidermal growth factor receptor 4; iNOS, inducible nitric oxide synthase; MMP1, matrix metalloproteinase-1; NF-κB, nuclear factor kappa B; NO, nitric oxide; NRG-1, neuregulin-1; O₂, molecular oxygen; O₂⁻, superoxide anion; ONOO⁻

, peroxynitrite; P, phosphoryl; PKC, protein kinase C; ROS, reactive oxygen species; α -SMA, α -smooth muscle actin; TGF- β , Transforming growth factor- β .

6. Molecular mechanisms modulated by doxorubicin and trastuzumab in fibroblasts

Myocardial fibrosis is a common feature of a wide diversity of cardiovascular pathologies including Dox- and trastuzumab-induced cardiotoxicity (155,156). Treatment with Dox induces the phenotypic transformation of cardiac fibroblasts into myofibroblasts, which synthesize large amounts of extracellular matrix (ECM) proteins, such as collagen (157). TGF- β /Smad signaling is the canonical pathway that mediates fibroblasts differentiation to myofibroblasts (158) and might be activated by ROS (159). Dox-induced ROS production in cardiomyocytes seems to activate this pathway and induce an aberrant repair process with the consequent release of large amounts of collagen and other components of the ECM (160). The upregulation of the signaling pathway substance P/neurokinin 1 receptor contributes to Dox adverse cardiac fibrosis (156). Substance P is known to induce hyperplastic response of adult cardiac fibroblasts, which is highly related with changes in redox and calcium homeostasis (161). Metalloproteinases (MMPs) contribute to Dox effects once they are involved in the degradation of ECM proteins (162). In fact, it was reported that in cardiac fibroblasts the content of MMP1 increases after Dox treatment (157). MMP1 upregulation promotes excessive ECM turnover, resulting in fibrosis and loss of heart function (163) (Figure 4).

Treatment with trastuzumab also promotes cardiac fibrosis (107); nevertheless, it was observed 7 days after treatment in a murine model (164). These profibrotic effects seem to be associated with the burst of proinflammatory cytokines (165), in a process induced by ROS derived from cardiomyocytes. One of these cytokines is TGF- β , which promotes the differentiation of fibroblasts into myofibroblasts (166), similarly to the reported for Dox (Figure 4). ECM overproduction interrupts the electrophysiological functions of the heart, leading to cardiac dysfunction (167).

7. Molecular mechanisms modulated by doxorubicin and trastuzumab in leukocytes

Dox and trastuzumab modulate the immune system with impact on cardiovascular homeostasis. Dox treatment was associated with the increased expression of iNOS in

leukocytes (168), a NOS isoform also present in cardiomyocytes (169). Indeed, Dox is a strong iNOS inducer by favoring the activation of NF- κ B and its translocation to the nucleus where activates the transcription of the *iNOS* gene (168). Increased iNOS expression leads to excessive •NO production (170). Thus, increased levels of peroxynitrite are expected (Figure 4).

As an antibody, one of the major mechanisms of trastuzumab effect is to attract immune cells towards cancer cell overexpressing HER2 (171). Then, immune cells release substances that kill the target cells (107). Since adults' cardiomyocytes express HER2, the cardiac effects of trastuzumab could also be potentiated by ADCC (Figure 4).

8. Concluding remarks

Standard care for HER2 positive BC cancer patients includes the combination of Dox and trastuzumab, whose clinical use is hampered by cardiotoxic side effects. Each of these antineoplastic therapies induce damage towards the myocardium once it activates several signaling pathways harbored not only in cardiomyocytes but in other cell types such as cardiac progenitor cells, endothelial cells, fibroblasts, and leukocytes. Thus, their combination is expected to be more stressful for the heart, ultimately leading to the impairment of the cardiac function. However, the molecular pathways underlying the cardiotoxic effect of the combined use of Dox and trastuzumab are still not completely understood and are not as clear as was expected earlier on. In fact, most of the studies focus on the signaling pathways modulated by each one of these therapies and rely on *in vitro* or animal models, and then make assumptions on possible relations.

The in-deep review provided in this paper on the molecular mechanisms modulated by Dox and trastuzumab in heart cells intends to feed future studies aiming to increase the understanding of the cardiotoxicity underlying the combined use of these drugs. Such knowledge is essential for the identification of specific biomarkers for the early detection of cardiac events and to develop strategies to counteract the cardiotoxicity of these anticancer therapies.

References

1. Miller KD, Nogueira L, Mariotto AB, Rowland JH, Yabroff KR, Alfano CM, Jemal A, Kramer JL, Siegel RL. Cancer treatment and survivorship statistics, 2019. *CA: A Cancer Journal for Clinicians*. 2019, 69:363–85.
2. Falzone L, Salomone S, Libra M. Evolution of cancer pharmacological treatments at the turn of the third millennium. *Frontiers in Pharmacology*. 2018, 9:1-26.
3. Gegechkori N, Haines L, Lin JJ. Long-Term and Latent Side Effects of Specific Cancer Types. *Medical Clinics of North America*. 2017, 101:1053–73.
4. Bodai BI, Tusso P. Breast cancer survivorship: a comprehensive review of long-term medical issues and lifestyle recommendations. *The Permanente Journal*. 2015, 19:48–79.
5. Barish R, Lynce F, Unger K, Barac A. Management of Cardiovascular Disease in Women with Breast Cancer. *Circulation*. 2019, 139:1110–20.
6. Perez IE, Taveras Alam S, Hernandez GA, Sancassani R. Cancer Therapy-Related Cardiac Dysfunction: An Overview for the Clinician. *Clinical Medicine Insights: Cardiology*. 2019, 13:1-11.
7. Yeh ETH, Bickford CL. Cardiovascular complications of cancer therapy: incidence, pathogenesis, diagnosis, and management. *Journal of the American College of Cardiology*. 2009, 53:2231–2247.
8. Pokrzywinski KL, Biel TG, Rosen ET, Bonanno JL, Aryal B, Mascia F, Moshkelani D, Mog S, Rao VA. Doxorubicin-induced cardiotoxicity is suppressed by estrous-staged treatment and exogenous 17β -estradiol in female tumor-bearing spontaneously hypertensive rats. *Biology of Sex Differences*. 2018, 9:1-17.
9. Ghigo A, Li M, Hirsch E. New signal transduction paradigms in anthracycline-induced cardiotoxicity. *BBA - Molecular Cell Research*. 2016, 1863:1916-25.
10. Volkova M, Russell R. Anthracycline Cardiotoxicity: Prevalence, Pathogenesis and Treatment. *Current Cardiology Reviews*. 2012, 7:214–20.
11. Chatterjee K, Zhang J, Honbo N, Karliner JS. Doxorubicin cardiomyopathy. *Cardiology*. 2010, 115:155–62.
12. Hoff DDV, Layard MW, Basa P, Davis HL, Hoff ALV, Rozencweig M, Muggia FM. Risk factors for doxorubicin-induced congestive heart failure. *Annals of Internal Medicine*. 1979, 91:710–7.

13. Cai F, Luis MAF, Lin X, Wang M, Cai L, Cen C, Biskup E. Anthracycline - induced cardiotoxicity in the chemotherapy treatment of breast cancer : Preventive strategies and treatment (Review). *Molecular and Clinical Oncology*. 2019, 11:15-23.
14. Schirmacher V. From chemotherapy to biological therapy: A review of novel concepts to reduce the side effects of systemic cancer treatment. *International Journal of Oncology*. 2019, 54:407–19.
15. Slamon DJ, Leyland-Jones B, Shak S, Fuchs H, Paton V, Bajamonde A, Fleming T, Eiermann W, Wolter J, Pegram M, Baselga J, Norton L. Use of chemotherapy plus a monoclonal antibody against her2 for metastatic breast cancer that overexpresses her2. *The New England Journal of Medicine*. 2001, 344:783–92.
16. Menna P, Minotti G, Salvatorelli E. Cardiotoxicity of Targeted Cancer Drugs: Concerns, “The Cart Before the Horse,” and Lessons from Trastuzumab. *Current Cardiology Reports*. 2019, 21:1-10.
17. Baselga J, Norton L, Albanell J, Kim YM, Mendelsohn J. Recombinant humanized anti-HER2 antibody (herceptin(TM)) enhances the antitumor activity of paclitaxel and doxorubicin against HER2/neu overexpressing human breast cancer xenografts. *Cancer Research*. 1998, 58:2825–31.
18. Cobleigh MA, Vogel CL, Tripathy D, Robert NJ, Scholl S, Fehrenbacher L, Wolter JM, Paton V, Shak S, Lieberman G, Slamon DJ. Multinational Study of the efficacy and safety of humanized anti- HER 2 Monoclonal antibody in woman who have HER2-overexpressing metastatic breast cancer. *Journal of Clinical Oncology*. 1999, 17:2639–48.
19. Pietras RJ, Poen JC, Gallardo D, Wongvipat PN, Lee HJ, Slamon DJ. Monoclonal antibody to HER-2/neu receptor modulates repair of radiation- induced DNA damage and enhances radiosensitivity of human breast cancer cells overexpressing this oncogene. *Cancer Research*. 1999, 59:1347–55.
20. Zeglinski M, Ludke A, Jassal DS, Singal PK. Trastuzumab-induced cardiac dysfunction: A “dual-hit.” *Experimental Clinical Cardiololgy*. 2011, 16:70-74.
21. Gunturu KS, Woo Y, Beaubier N, Remotti HE, Saif MW. Gastric cancer and trastuzumab: First biologic therapy in gastric cancer. *Therapeutic Advances in Medical Oncology*. 2013, 5:143–51.
22. Yang D, Hendifar A, Lenz C, Togawa K, Lenz F, Lurje G, Pohl A, Winder T, Ning

- Y, Groshen S, Lenz HJ. Survival of metastatic gastric cancer: Significance of age, sex and race/ethnicity. *Journal of Gastrointestinal Oncology*. 2011, 2:77–84.
23. Tarantini L, Cioffi G, Gori S, Tuccia F, Boccardi L, Bovelli D, Lestuzzi C, Maurea N, Oliva S, Russo G, Faggiano P. Trastuzumab adjuvant chemotherapy and cardiotoxicity in real-world women with breast cancer. *Journal of Cardiac Failure*. 2012, 18:113–119.
 24. Newsheen S, Viscuse P V., O’Sullivan CC, Sandhu NP, Haddad TC, Blaes A, Klemp J, Nholo L, Herrmann J, Ruddy KJ. Incidence, Diagnosis, and Treatment of Cardiac Toxicity From Trastuzumab in Patients With Breast Cancer. *Current Breast Cancer Reports*. 2017, 9:173–82.
 25. Maximiano S, Magalhães P, Guerreiro MP, Morgado M. Trastuzumab in the Treatment of Breast Cancer. *BioDrugs*. 2016, 30:75-86.
 26. Peetla C, Bhave R, Vijayaraghavalu S, Stine A, Kooijman E, Labhasetwar V. Drug resistance in breast cancer cells: Biophysical characterization of and doxorubicin interactions with membrane lipids. *Molecular Pharmaceutics*. 2010, 7:2334–48.
 27. Muley H, Fadó R, Rodríguez-Rodríguez R, Casals N. Drug uptake-based chemoresistance in breast cancer treatment. *Biochemical Pharmacology*. 2020, 177:1-14.
 28. Sagwal SK, Pasqual-Melo G, Bodnar Y, Gandhirajan RK, Bekeschus S. Combination of chemotherapy and physical plasma elicits melanoma cell death via upregulation of SLC22A16. *Cell Death and Disease*. 2018, 9:1-13.
 29. Nebigil CG, Désaubry L. Updates in anthracycline-mediated cardiotoxicity. *Frontiers in Pharmacology*. 2018, 9:1–13.
 30. Zhao L, Zhang B. Doxorubicin induces cardiotoxicity through upregulation of death receptors mediated apoptosis in cardiomyocytes. *Scientific Reports*. 2017, 7:1-11.
 31. Huang KM, Hu S, Sparreboom A. Drug transporters and anthracycline-induced cardiotoxicity. *Pharmacogenomics*. 2018, 19:883–8.
 32. Guo W, Song Y, Song W, Liu Y, Liu Z, Zhang D Tang Z, Bai O. Co-delivery of Doxorubicin and Curcumin with Polypeptide Nanocarrier for Synergistic Lymphoma Therapy. *Scientific Reports*. 2020, 10:1–16.
 33. Nitiss JL. Targeting DNA topoisomerase II in cancer chemotherapy. *Nature Reviews Cancer*. 2009, 9:338-350.

34. Goffart S, Hangan A, Pohjoismäki JLO. Twist and turn—topoisomerase functions in mitochondrial DNA maintenance. *International Journal of Molecular Sciences*. 2019, 20:1-17.
35. Sawyer DB. Anthracyclines and Heart Failure. *The New England Journal of Medicine*. 2018, 368:1154-1156.
36. Ashley N, Poulton J. Mitochondrial DNA is a direct target of anti-cancer anthracycline drugs. *Biochemical and Biophysical Research Communications*. 2009, 378:450–5.
37. Renu K, V.G. A, Tirupathi TP, Arunachalam S. Molecular Mechanism of Doxorubicin-Induced Cardiomyopathy – An Update. *European Journal of Pharmacology*. 2018, 818:241-253.
38. Ginzac A, Passildas J, Gadéa E, Abrial C, Molnar I, Trésorier R, Duclos M, Thivat E, Durando X. Treatment-Induced Cardiotoxicity in Breast Cancer: A Review of the Interest of Practicing a Physical Activity. *Oncology*. 2019, 96:223-234.
39. Kalyanaraman B. Teaching the basics of the mechanism of doxorubicin-induced cardiotoxicity: Have we been barking up the wrong tree? *Redox Biology*. 2019, 1-18.
40. Gonzalez Y, Pokrzywinski KL, Rosen ET, Mog S, Aryal B, Chehab LM, Vijay V, Moland CL, Desai VG, Dickey JS, Rao VA. Reproductive hormone levels and differential mitochondria-related oxidative gene expression as potential mechanisms for gender differences in cardiosensitivity to Doxorubicin in tumor-bearing spontaneously hypertensive rats. *Cancer Chemotherapy and Pharmacology*. 2015, 76:447-459.
41. Hrynychak I, Sousa E, Pinto M, Costa VM. The importance of drug metabolites synthesis: the case-study of cardiotoxic anticancer drugs. *Drug Metabolism Reviews*. 2017, 49:158-196.
42. Santos DS dos, Goldenberg RC dos S. Doxorubicin-Induced Cardiotoxicity: From Mechanisms to Development of Efficient Therapy. *Cardiotoxicity*. 2018, 1:3-24.
43. Canzoneri JC, Oyelere AK. Interaction of anthracyclines with iron responsive element mRNAs. *Nucleic Acids Research*. 2008, 36:6825-6834.
44. Xu X, Persson HL, Richardson DR. Molecular pharmacology of the interaction of anthracyclines with iron. *Molecular Pharmacology*. 2005, 68:261–71.
45. Reis-Mendes A, Carvalho F, Remião F, Sousa E, Bastos MDL, Costa VM. The main

- metabolites of fluorouracil + adriamycin + cyclophosphamide (FAC) are not major contributors to FAC toxicity in H9C2 cardiac differentiated cells. *Biomolecules*. 2019, 9:1-20.
46. Reis-Mendes AF, Sousa E, de Lourdes Bastos M, Marisa Costa V. The Role of the Metabolism of Anticancer Drugs in Their Induced-Cardiotoxicity. *Current Drug Metabolism*. 2015, 17:75–90.
 47. Minotti G, Salvatorelli E, Menna P, Ronchi R, Cairo G. Doxorubicin irreversibly inactivates iron regulatory proteins 1 and 2 in cardiomyocytes: Evidence for distinct metabolic pathways and implications for iron-mediated cardiotoxicity of antitumor therapy. *Cancer Research*. 2001, 61:8422-8428.
 48. Minotti G, Recalcati S, Mordente A, Liberi G, Calafiore AM, Mancuso C, Preziosi P, Cairo G. The secondary alcohol metabolite of doxorubicin irreversibly inactivates aconitase/iron regulatory protein-1 in cytosolic fractions from human myocardium. *FASEB Journal*. 1998, 12:541-552.
 49. Wu J, Hong H, Ji H, Wang YY, Wang Y, Li YQ, Li WG, Long Y, Xia YZ. Glutathione depletion upregulates P-glycoprotein expression at the blood-brain barrier in rats. *Journal of Pharmacy and Pharmacology*. 2009, 61:819-824.
 50. Deng J, Coy D, Zhang W, Sunkara M, Morris AJ, Wang C, Chaiswing L, Clair DS, Vore M, jungsuwadee P. Elevated glutathione is not sufficient to protect against doxorubicin-induced nuclear damage in heart in multidrug resistance-associated Protein 1 (Mrp1/Abcc1) null mice. *Journal of Pharmacology and Experimental Therapeutics*. 2015, 355:272-279.
 51. Lee KF, Simon H, Chen H, Bates B, Hung MC, Hauser C. Requirement for neuregulin receptor erbB2 in neural and cardiac development. *Nature*. 1995, 378:667-668.
 52. Vasti C, Hertig CM. Neuregulin-1/erbB activities with focus on the susceptibility of the heart to anthracyclines. *World Journal of Cardiology*. 2014, 6:653-662.
 53. Liu FF, Stone JR, Schuld AJT, Okoshi K, Okoshi MP, Nakayama M, Ho KKL, Manning WJ, Marchionni MA, Lorell BH, Morgan JP, Yan X. Heterozygous knockout of neuregulin-1 gene in mice exacerbates doxorubicin-induced heart failure. *American Journal Physiology. Heart and Circulatory Physiology*. 2005, 289:H660-H666.
 54. Gabrielson K, Bedja D, Pin S, Tsao A, Gama L, Yuan B, Muratore N. Heat shock

- protein 90 and ErbB2 in the cardiac response to doxorubicin injury. *Cancer Research*. 2007, 67:1436–41.
55. Baliga RR, Pimental DR, Zhao YY, Simmons WW, Marchionni MA, Sawyer DB, Kelly RA. NRG-1 - induced cardiomyocyte hypertrophy. Role of PI-3-kinase , p70 S6K , and MEK-MAPK-RSK. *The American Journal of Physiology*. 2018, 277:H2026-H2037.
 56. Belmonte F, Das S, Sysa-Shah P, Sivakumaran V, Stanley B, Guo X, Paolocci N, Aon MA, Nagane M, Kuppusamy P, Steenbergen C, Gabrielson K. ErbB2 overexpression upregulates antioxidant enzymes, reduces basal levels of reactive oxygen species, and protects against doxorubicin cardiotoxicity. *American Journal of Physiology - Heart Circulatory Physiology*. 2015, 309:H1271-H1280.
 57. Octavia Y, Tocchetti CG, Gabrielson KL, Janssens S, Crijns HJ, Moens AL. Doxorubicin-induced cardiomyopathy: From molecular mechanisms to therapeutic strategies. *Journal of Molecular and Cellular Cardiology*. 2012, 52:1213-1225.
 58. Sánchez A, Martínez P, Muñoz M, Benedito S, García-Sacristán A, Hernández M, Prieto D. Endothelin-1 contributes to endothelial dysfunction and enhanced vasoconstriction through augmented superoxide production in penile arteries from insulin-resistant obese rats: Role of ETA and ETB receptors. *British Journal of Pharmacology*. 2014, 171:5682-5695.
 59. Suzuki T, Kumazaki T, Mitsui Y. Endothelin-1 is produced and secreted by neonatal rat cardiac myocytes *in vitro*. *Biochemical and Biophysical Research Communications*. 1993, 191:823-830.
 60. Moravec CS, Reynolds EE, Stewart RW, Bond M. Endothelin is a positive inotropic agent in human and rat heart *in vitro*. *Biochemical and Biophysical Research Communications*. 1989, 159:14-18.
 61. Suzuki T, Hoshi H, Sasaki H, Mitsui Y. Endothelin-1 stimulates hypertrophy and contractility of neonatal rat cardiac myocytes in a serum-free medium. *Journal of Cardiovascular Pharmacology*. 1991, 17:S182-S186.
 62. Mitry MA, Edwards JG. Doxorubicin induced heart failure: Phenotype and molecular mechanisms. *IJC Heart and Vasculature*. 2016, 10:17–24.
 63. Bien S, Riad A, Ritter CA, Gratz M, Olshausen F, Westermann D, Grube M, Krieg T, Ciecholewski S, Felix SB, Staudt A, Schultheiss HP, Ewert R, Volker U, Tschope C,

- Kroemer HK. The endothelin receptor blocker bosentan inhibits doxorubicin-induced cardiomyopathy. *Cancer Research*. 2007, 67:10428–35.
64. Dorn GW. Mitochondrial dynamics in heart disease. *Biochimica et Biophysica Acta - Molecular Cell Research*. 2013, 1833:233-241.
 65. Sokolove PM. Interactions of Adriamycin aglycones with mitochondria may mediate Adriamycin cardiotoxicity. *International Journal of Biochemistry*. 1994, 26:1341–50.
 66. Guven C, Sevgiler Y, Taskin E. Mitochondrial Dysfunction Associated with Doxorubicin. *Mitochondrial Diseases*. 2018, 13:323-360.
 67. Dudek J, Hartmann M, Rehling P. The role of mitochondrial cardiolipin in heart function and its implication in cardiac disease. *Biochimica et Biophysica Acta - Molecular Basis of Disease*. 2019, 1865:810–21.
 68. Aryal B, Rao VA. Deficiency in cardiolipin reduces doxorubicin-induced oxidative stress and mitochondrial damage in human B-lymphocytes. *PLoS One*. 2016, 11:1-20.
 69. Gorini S, De Angelis A, Berrino L, Malara N, Rosano G, Ferraro E. Chemotherapeutic Drugs and Mitochondrial Dysfunction: Focus on Doxorubicin, Trastuzumab, and Sunitinib. *Oxidative Medicine and Cellular Longevity*. 2019, 2019:1-15.
 70. He H, Wang L, Qiao Y, Zhou Q, Li H, Chen S, Yin D, Huang Q, He M. Doxorubicin induces endotheliotoxicity and mitochondrial dysfunction via ROS/eNOS/NO pathway. *Frontiers in Pharmacology*. 2019, 10:1-16.
 71. Childs AC, Phaneuf SL, Dirks AJ, Phillips T, Leeuwenburgh C. Doxorubicin Treatment in Vivo Causes Cytochrome *c* Release and Cardiomyocyte Apoptosis, As Well As Increased Mitochondrial Efficiency, Superoxide Dismutase Activity, and Bcl-2:Bax Ratio. *Cancer Research*. 2002, 62:4592-4598.
 72. Nemoto S, Sheng Z, Lin A. Opposing Effects of Jun Kinase and p38 Mitogen-Activated Protein Kinases on Cardiomyocyte Hypertrophy. *Molecular and Cellular Biology*. 1998, 18:3518-3526.
 73. Kim DS, Woo ER, Chae SW, Ha KC, Lee GH, Hong ST, Kwon DY, Kim MS, Jung YK, Kim HM, Kim HK, Kim HR, Chae HJ. Plantainoside D protects adriamycin-induced apoptosis in H9c2 cardiac muscle cells via the inhibition of ROS generation and NF- κ B activation. *Life Sciences*. 2007, 80:314-323.
 74. Park AM, Nagase H, Liu L, Kumar SV, Szwergold N, Wong CM, Suzuki YJ.

- Mechanism of anthracycline-mediated down-regulation of GATA4 in the heart. *Cardiovascular Research*. 2011, 90:97-104.
75. Wang S, Leonard SS, Ye J, Ding M, Shi X. The role of hydroxyl radical as a messenger in Cr(VI)-induced p53 activation. *American Journal of Physiology - Cell Physiology*. 2000, 279:868-875.
76. Ueno M, Kakinuma Y, Yuhki KI, Murakoshi N, Iemitsu M, Miyauchi T, Yamaguchi I. Doxorubicin induces apoptosis by activation of caspase-3 in cultured cardiomyocytes in vitro and rat cardiac ventricles in vivo. *Journal of Pharmacological Sciences*. 2006, 101:151-158.
77. Ferreira R, Nogueira-ferreira R, Trindade F, Powers SK, Moreira-gonçalves D. Sugar or fat: the metabolic choice of the trained heart. *Metabolism*. 2018, 87:98-104.
78. Tokarska-Schlattner M, Zaugg M, Da Silva R, Lucchinetti E, Schaub MC, Wallimann T, Schlattner U. Acute toxicity of doxorubicin on isolated perfused heart: Response of kinases regulating energy supply. *American Journal of Physiology - Heart Circulatory Physiology*. 2005, 289:H37-H47.
79. Wang S, Song P, Zou M. Inhibition of AMP-activated Protein Kinase α (AMPK α) by Doxorubicin Accentuates Genotoxic Stress and Cell Death in Mouse Embryonic Fibroblasts and Cardiomyocytes. *The Journal of Biological Chemistry*. 2012, 287:8001-8012.
80. Moulin M, Piquereau J, Mateo P, Fortin D, Rucker-Martin C, Gressette M, Lefebvre F, Gresikova M, Solgadi A, Veksler V, Garnier A, Ventura-Clapier R. Sexual Dimorphism of Doxorubicin-Mediated Cardiotoxicity: Potential Role of Energy Metabolism Remodeling Potential Role of Energy Metabolism Remodeling. *Circulation Heart Failure*. 2015, 8:98-108.
81. Kay L, Potenza L, Seffouh A, Schnebelen C, Sestili P, Schlattner U, Tokarska-Schlattner M. Inhibition of AMPK signalling by doxorubicin : at the crossroads of the cardiac responses to energetic, oxidative, and genotoxic stress. *Cardiovascular Research*. 2012, 94:290–9.
82. Shabalala S, Louw J, Muller CJF, Johnson R. Polyphenols, autophagy and doxorubicin-induced cardiotoxicity. *Life Sciences*. 2017, 180:160–70.
83. Koleini N, Kardami E. Autophagy and mitophagy in the context of doxorubicin-induced cardiotoxicity. *Oncotarget*. 2017, 8:46663–80.

84. Kim KH, Lee MS. Autophagy - A key player in cellular and body metabolism. *Nature Reviews Endocrinology*. 2014, 10:322–37.
85. Wang X, Wang XL, Chen HL, Wu D, Chen JX, Wang XX, Li RL, He JH, Mo L, Cen X, Wei YQ, Jiang W. Ghrelin inhibits doxorubicin cardiotoxicity by inhibiting excessive autophagy through AMPK and p38-MAPK. *Biochemical Pharmacology*. 2014, 88:334–50.
86. Kawaguchi T, Takemura G, Kanamori H, Takeyama T, Watanabe T, Morishita K, Ogino A, Tsujimoto A, Goto K, Maruyama R, Kawasaki M, Mikami A, Fujiwara T, Fujiwara H, Minatoguchi S. Prior starvation mitigates acute doxorubicin cardiotoxicity through restoration of autophagy in affected cardiomyocytes. *Cardiovasc Research*. 2012, 96:456–65.
87. Xu X, Chen K, Kobayashi S, Timm D, Liang Q. Resveratrol attenuates doxorubicin-induced cardiomyocyte death via inhibition of p70 S6 kinase 1-mediated autophagy. *The Journal of Pharmacology and Experimental Therapeutics*. 2012, 341:183–95.
88. Gu J, Hu W, Song ZP, Chen YG, Zhang DD, Wang CQ. Resveratrol-induced autophagy promotes survival and attenuates doxorubicin-induced cardiotoxicity. *International Immunopharmacology*. 2016, 32:1–7.
89. Xu X, Bucala R, Ren J. Macrophage migration inhibitory factor deficiency augments doxorubicin-induced cardiomyopathy. *Journal of the American Heart Association*. 2013, 2:1–18.
90. Cao Y, Shen T, Huang X, Lin Y, Chen B, Pang J, Li G, Wang Q, Zohrabian S, Duan C, Ruan Y, Man Y, Wang S, Li J. Astragalus polysaccharide restores autophagic flux and improves cardiomyocyte function in doxorubicin-induced cardiotoxicity. *Oncotarget*. 2017, 8:4837–48.
91. Li DL, Wang ZV, Ding G, Tan W, Luo X, Criollo A, Xie M, Jiang N, May H, Kyrychenko V, Schneider JW, Gillette TG, Hill JA. Doxorubicin Blocks Cardiomyocyte Autophagic Flux by Inhibiting Lysosome Acidification. *Circulation*. 2016, 133:1668–87.
92. Yin J, Guo J, Zhang Q, Cui L, Zhang L, Zhang T, Zhao J, Li J, Middleton A, Carmichael PL, Peng S. Doxorubicin-induced mitophagy and mitochondrial damage is associated with dysregulation of the PINK1/parkin pathway. *Toxicology in Vitro*. 2018, 51:1–10.

93. Du Q, Zhu B, Zhai Q, Yu B. Sirt3 attenuates doxorubicin-induced cardiac hypertrophy and mitochondrial dysfunction via suppression of Bnip3. *American Journal of Translational Research*. 2017, 9:3360–73.
94. Narendra DP, Jin SM, Tanaka A, Suen DF, Gautier CA, Shen J, Cookson MR, Youle RJ. PINK1 is selectively stabilized on impaired mitochondria to activate Parkin. *PLoS Biology*. 2010, 8:1-21.
95. Matsuda N, Sato S, Shiba K, Okatsu K, Saisho K, Gautier CA, Sou YS, Saiki S, Kawajiri S, Soto F, Kimura M, Komatsu M, Hattori N, Tanaka K. PINK1 stabilized by mitochondrial depolarization recruits Parkin to damaged mitochondria and activates latent Parkin for mitophagy. *Journal of Cell Biology*. 2010, 189:211–21.
96. Hull TD, Boddu R, Guo L, Tisher CC, Traylor AM, Patel B, Joseph R, Prabhu SD, Suliman HB, Piantadosi CA, Agarwal A, George JF. Heme oxygenase-1 regulates mitochondrial quality control in the heart. *JCI Insight*. 2016, 1:1-17.
97. Dhingra R, Margulets V, Chowdhury SR, Thliveris J, Jassal D, Fernyhough P, Dorn GW, Kirshenbaum LA. Bnip3 mediates doxorubicin-induced cardiac myocyte necrosis and mortality through changes in mitochondrial signaling. *Proceedings of the National Academy of Sciences of the United States of America*. 2014, 111:E5537–44.
98. Wu NN, Zhang Y, Ren J. Mitophagy, Mitochondrial Dynamics, and Homeostasis in Cardiovascular Aging. *Oxidative Medicine and Cellular Longevity*. 2019, 2019:1–15.
99. Deschamps AM, Murphy E. Activation of a novel estrogen receptor, GPER, is cardioprotective in male and female rats. *American Journal of Physiology - Heart and Circulatory Physiology*. 2009, 297:1806-1813.
100. Urata Y, Ihara Y, Murata H, Goto S, Koji T, Yodoi J, Inoue S, Kondo T. 17 β -estradiol protects against oxidative stress-induced cell death through the glutathione/glutaredoxin-dependent redox regulation of Akt in myocardial H9c2 cells. *The Journal of Biological Chemistry*. 2006, 281:13092–102.
101. Lin DY, Tsai FJ, Tsai CH, Huang CY. Mechanisms governing the protective effect of 17 β -estradiol and estrogen receptors against cardiomyocyte injury. *Biomedicine*. 2011, 1:21-28.
102. Muñoz-Castañeda JR, Montilla P, Muñoz MC, Bujalance I, Muntané J, Túnez I. Effect of 17- β -estradiol administration during adriamycin-induced cardiomyopathy in

- ovariectomized rat. *European Journal Pharmacology*. 2005, 523:86-92.
103. Rattanasopa C, Kirk JA, Bupha-Intr T, Papadaki M, Tombe PP, Wattanapermpool J. Estrogen but not testosterone preserves myofilament function from doxorubicin-induced cardiotoxicity by reducing oxidative modifications. *American Journal of Physiology - Heart and Circulatory Physiology*. 2018, 2:6-11.
 104. Jiang N, Lin JJ, Wang J, Zhang BN, Li A, Chen ZY, Guo S, Li BB, Duan YZ, Yan RY, Yan HF, Fu XY, Zhou JL, Yang HM, Cui Y. Novel treatment strategies for patients with HER2-positive breast cancer who do not benefit from current targeted therapy drugs (Review). *Experimental and Therapeutic Medicine*. 2018, 16:2183-2192.
 105. Osoba D, Slamon DJ, Burchmore M, Murphy M. Effects on quality of life of combined trastuzumab and chemotherapy in women with metastatic breast cancer. *Journal of Clinical Oncology*. 2002, 20:3106-3113.
 106. Pondé NF, Lambertini M, De Azambuja E. Twenty years of anti-HER2 therapy-associated cardiotoxicity. *ESMO Open*. 2016, 1:1-13.
 107. Mohan N, Jiang J, Dokmanovic M, Wu WJ. Trastuzumab-mediated cardiotoxicity: current understanding, challenges, and frontiers. *Antibody Therapeutics*. 2018, 1:13-17.
 108. Florido R, Smith KL, Cuomo KK, Russell SD. Cardiotoxicity From Human Epidermal Growth Factor Receptor-2 (HER2) Targeted Therapies. *Journal of the American Heart Association*. 2017, 6:1-15.
 109. Lemmens K, Doggen K, De Keulenaer GW. Role of neuregulin-1/ErbB signaling in cardiovascular physiology and disease: Implications for therapy of heart failure. *Circulation*. 2007, 116:954-960.
 110. Chang F, Steelman LS, Lee JT, Shelton JG, Navolanic PM, Blalock WL, Franklin RA, McCubrey JA. Signal transduction mediated by the Ras/Raf/MEK/ERK pathway from cytokine receptors to transcription factors: Potential targeting for therapeutic intervention. *Leukemia*. 2003, 17:1263-1293.
 111. Mebratu Y, Tesfaigzi Y. How ERK1/2 activation controls cell proliferation and cell death is subcellular localization the answer? *Cell Cycle*. 2009, 8:1168-1175.
 112. Yin H-K. Progress in neuregulin/ErbB signaling and chronic heart failure. *World Journal of Hypertension*. 2015, 5:63-73.

113. Manning BD, Toker A. AKT/PKB Signaling: Navigating the Network. *Cell*. 2017, 169:381-405.
114. Miyamoto S, Murphy AN, Brown JH. Akt mediated mitochondrial protection in the heart: Metabolic and survival pathways to the rescue. *Journal of Bioenergetics and Biomembranes*. 2009, 41:169-180.
115. Laird-Fick HS, Tokala H, Kandola S, Kehdi M, Pelosi A, Wang L, Grondahl B. Early morphological changes in cardiac mitochondria after subcutaneous administration of trastuzumab in rabbits: possible prevention with oral selenium supplementation. *Cardiovascular Pathology*. 2020, 44:107159.
116. Dobner S, Amadi OC, Lee RT. Cardiovascular Mechanotransduction. *Muscle*. 2012, 1:173-186.
117. Nemeth BT, Varga ZV, Wu WJ, Pacher P. Trastuzumab cardiotoxicity: from clinical trials to experimental studies. *British Journal of Pharmacology*. 2017, 174:3727-3748.
118. Jerusalem G, Lancellotti P, Bae S. HER2 + breast cancer treatment and cardiotoxicity : monitoring and management American Society of Clinical Oncology European Society of Cardiology. *Breast Cancer Research and Treatment*. 2019, 177:237-250.
119. Gianni L, Salvatorelli E, Minotti G. Anthracycline cardiotoxicity in breast cancer patients: Synergism with trastuzumab and taxanes. *Cardiovascular Toxicology*. 2007, 7:67-71.
120. Jiang J, Mohan N, Endo Y, Shen Y, Wu WJ. Type IIB DNA topoisomerase is downregulated by trastuzumab and doxorubicin to synergize cardiotoxicity. *Oncotarget*. 2018, 9:3075–3075.
121. Kertmen N, Aksoy S, Uner A, Sargon M, Ozkayar O, Keskin O, Babacan T, Sarici F, Sendur MA, Arik Z, Akin S, Altundag K. Which sequence best protects the heart against trastuzumab and anthracycline toxicity? an electron microscopy study in rats. *Anticancer Research*. 2015, 35:857–64.
122. Huszno J, Badora A, Nowara E. The influence of steroid receptor status on the cardiotoxicity risk in HER2-positive breast cancer patients receiving trastuzumab. *Archives of Medical Science*. 2015, 11:371-377.
123. Zablocki D, Sadoshima J. Angiotensin II and oxidative stress in the failing heart.

- Antioxidants Redox Signal*. 2013, 19:1095-1109.
124. Angelis A, Urbanek K, Cappetta D, Piegari E, Ciuffreda LP, Rivellino A, Russo R, Esposito G, Rossi F, Berrino L. Doxorubicin cardiotoxicity and target cells: a broader perspective. *Cardio-Oncology*. 2016, 2:1–8.
 125. Savi M, Bocchi L, Rossi S, Frati C, Graiani G, Lagrasta C, Miragoli M, Pasquale ED, Stirparo GG, Mastrototaro G, Urbanek K, Angelis AD, Macchi E, Stilli D, Quaini F, Musso E. Antiarrhythmic effect of growth factor-supplemented cardiac progenitor cells in chronic infarcted heart. *American Journal of Physiology - Heart and Circulatory Physiology*. 2016, 310:H1622–48.
 126. Huang C, Zhang X, Ramil JM, Rikka S, Kim L, Lee Y, Gude NA, Thistlethwaite PA, Sussman MA, Gottlieb RA, Gustafsson AB. Juvenile Exposure to Anthracyclines Impairs Cardiac Progenitor Cell Function and Vascularization Resulting in Greater Susceptibility to Stress-Induced Myocardial Injury in Adult Mice. *Circulation*. 2015, 676-683.
 127. Angelis A, Piegari E, Cappetta D, Russo R, Esposito G, Ciuffreda LP, Ferraiolo FAV, Frati C, Fagnoni F, Berrino L, Quaini F, Rossi F, Urbanek K. SIRT1 activation rescues doxorubicin-induced loss of functional competence of human cardiac progenitor cells. *International Journal of Cardiology*. 2015, 189:30–44.
 128. Piegari E, Angelis AD, Cappetta D, Russo R, Esposito G, Costantino S, Graiani G, Frati C, Prezioso L, Berrino L, Urbanek K, Quaino F, Rossi F. Doxorubicin induces senescence and impairs function of human cardiac progenitor cells. *Basic Research in Cardiology*. 2013, 108:1-18.
 129. Angelis AD, Piegari E, Cappetta D, Marino L, Filippelli A, Berrino L, Ferreira-Martins J, Zheng H, Hosoda T, Rota M, Urbanek K, Kajstura J, Leri A, Rossi F, Anversa P. Anthracycline Cardiomyopathy Is Mediated by Depletion of the Cardiac Stem Cell Pool and Is Rescued by Restoration of Progenitor Cell Function. *Circulation*. 2010, 19:276-92.
 130. Abushouk AI, Muhammad A, Salem A, Saad A, Afifi AM, Afify AY, Afify H, Salem HSE, Ghanem E, Abdel-Daim MM. Mesenchymal Stem Cell Therapy for Doxorubicin-Induced Cardiomyopathy: Potential Mechanisms, Governing Factors, and Implications of the Heart Stem Cell Debate. *Frontiers in Pharmacology*. 2019, 10:1–12.

131. Angelis A De, Cappetta D, Berrino L, Urbanek K. Doxorubicin Cardiotoxicity: Multiple Targets and Translational Perspectives. *Cardiotoxicity*. 2018, 26-46.
132. Fabbi P, Spallarossa P, Garibaldi S, Barisione C, Mura M, Altieri P, Rebesco B, Monti MG, Canepa M, Ghigliotti G, Brunelli C, Ameri P. Doxorubicin impairs the insulin-like growth factor-1 system and causes insulin-like growth factor-1 resistance in cardiomyocytes. *PLoS One*. 2015, 10:1–14.
133. Madonna R, Rokosh G, De Caterina R, Bolli R. Hepatocyte growth factor/met gene transfer in cardiac stem cells-potential for cardiac repair. *Basic Research in Cardiology*. 2010, 105:443–52.
134. Park JH, Choi SH, Kim H, Ji ST, Jang WB, Kim JH, Baik SH, Kwon SM. Doxorubicin regulates autophagy signals via accumulation of cytosolic Ca²⁺ in human cardiac progenitor cells. *International Journal of Molecular Sciences*. 2016, 17:1-13.
135. Denegri A, Moccetti T, Moccetti M, Spallarossa P, Brunelli C, Ameri P. Cardiac toxicity of trastuzumab in elderly patients with breast cancer. *Journal of Geriatric Cardiology*. 2016, 13:355-363.
136. Barth AS, Zhang Y, Li T, Smith RR, Chimenti I, Terrovitis I, Davis DR, Kizana E, Ho AS, O'Rourke B, Wolff AC, Gerstenblith G, Marbán E. Functional Impairment of Human Resident Cardiac Stem Cells by the Cardiotoxic Antineoplastic Agent Trastuzumab. *Stem Cells Translational Medicine*. 2012, 1:289–97.
137. Pinto AR, Ilinykh A, Ivey MJ, Kuwabara JT, D'antoni ML, Debuque R, Chandran A, Wang L, Arora K, Rosenthal N, Tallquist MD. Revisiting cardiac cellular composition. *Circulation Research*. 2016, 118:400–9.
138. Wilkinson EL, Sidaway JE, Cross MJ. Cardiotoxic drugs Herceptin and doxorubicin inhibit cardiac microvascular endothelial cell barrier formation resulting in increased drug permeability. *Biology Open*. 2016, 5:1362-1370.
139. Polonchuk L, Chabria M, Davies MJ, Gentile C. Doxorubicin-Mediated Toxic Effects Are Mediated Via NO/eNOS in a Novel 3D in Vitro Model of the Human Heart. *Free Radical Biology and Medicine*. 2016, 100:S142.
140. Vásquez-Virar J, Martasek P, Hogg N, Masters BSS, Pritchard KA, Kalyanaraman B. Endothelial Nitric Oxide Synthase-Dependent Superoxide Generation from Adriamycin. *Biochemistry*. 1997, 36:11293-11297.

141. Mukhopadhyay P, Rajesh M, Bátkai S, Kashiwaya Y, Haskó G, Liaudet L, Szabó C, Pacher P. Role of superoxide, nitric oxide, and peroxynitrite in doxorubicin-induced cell death in vivo and in vitro. *American Journal of Physiology - Heart and Circulatory Physiology*. 2009, 296:1466–83.
142. Pacher P, Beckman JS, Liaudet L. Nitric oxide and peroxynitrite in health and disease. *Physiological Reviews*. 2007, 87:315-424.
143. Peluffo G, Radi R. Biochemistry of protein tyrosine nitration in cardiovascular pathology. *Cardiovascular Research*. 2007, 75:291-302.
144. Mihm MJ, Yu F, Weinstein DM, Reiser PJ, Bauer JA. Intracellular distribution of peroxynitrite during doxorubicin cardiomyopathy: evidence for selective impairment of myofibrillar creatine kinase. *British Journal of Pharmacology*. 2002, 135:581-588.
145. Keltai K, Cervenak L, Makó V, Doleschall Z, Zsáry A, Karádi I. Doxorubicin selectively suppresses mRNA expression and production of endothelin-1 in endothelial cells. *Vascular Pharmacology*. 2010, 53:209–14.
146. Talman V, Kivelä R. Cardiomyocyte—Endothelial Cell Interactions in Cardiac Remodeling and Regeneration. *Frontiers in Cardiovascular Medicine*. 2018, 5:1–8.
147. Davenport AP, Hyndman KA, Dhaun N, Southan C, Kohan DE, Pollock JS, Pollock DM, Webb DJ, Maguire JJ. Endothelin. *Pharmacology Reviews*. 2016, 68:357-418.
148. Abukar Y, May CN, Ramchandra R. Role of endothelin-1 in mediating changes in cardiac sympathetic nerve activity in heart failure. *American Journal of Physiology - Regulatory Integrative and Comparative Physiology*. 2016, 310:94-99.
149. Mazzuca MQ, Khalil RA. Vascular endothelin receptor type B: Structure, function and dysregulation in vascular disease. *Biochemical Pharmacology*. 2012, 84:147–62.
150. Luu AZ, Chowdhury B, Al-Omran M, Teoh H, Hess DA, Verma S. Role of Endothelium in Doxorubicin-Induced Cardiomyopathy. *JACC Basic to Translational Science*. 2018, 3:861–70.
151. Sandoo A, Kitas GD, Carmichael AR. Endothelial dysfunction as a determinant of trastuzumab-mediated cardiotoxicity in patients with breast cancer. *Anticancer Research*. 2014, 34:1147-1151.
152. Sandoo A. Breast cancer therapy and cardiovascular risk: focus on trastuzumab. *Vascular Health and Risk Management*. 2015, 11:223-228.
153. Dugaucquier L, Feyen E, Mateiu L, Bruyns TAM, De Keulenaer GW, Segers VFM.

- The role of endothelial autocrine NRG1/ERBB4 signaling in cardiac remodeling. *American Journal of Physiology - Heart and Circulatory Physiology*. 2020, 319:H443–55.
154. Langbein H, Brunssen C, Hofmann A, Cimalla P, Brux M, Bornstein SR, Deussen A, Koch E, Morawietz H. NADPH oxidase 4 protects against development of endothelial dysfunction and atherosclerosis in LDL receptor deficient mice. *European Heart Journal*. 2016, 37:1753–61.
 155. Riccio G, Coppola C, Piscopo G, Capasso I, Maurea C, Esposito E, Lorenzo CD, Maurea N. Trastuzumab and target-therapy side effects: Is still valid to differentiate anthracycline Type I from Type II cardiomyopathies? *Human Vaccines Immunotherapeutics*. 2016, 12:1124–31.
 156. Levick SP, Soto-Pantoja DR, Bi J, Hundley WG, Widiapradja A, Manteufel EJ, Bradshaw TW, Meléndez GC. Doxorubicin-Induced Myocardial Fibrosis Involves the Neurokinin-1 Receptor and Direct Effects on Cardiac Fibroblasts. *Heart Lung and Circulation*. 2019, 28:1598–605.
 157. Narikawa M, Umemura M, Tanaka R, Hikichi M, Nagasako A, Fujita T, Yokoyama U, Ishigami T, Kimura K, Tamura K, Ishikawa Y. Doxorubicin induces trans-differentiation and MMP1 expression in cardiac fibroblasts via cell death-independent pathways. *PLoS One*. 2019, 14:1–17.
 158. Dobaczewski M, Bujak M, Li N, Gonzalez-Quesada C, Mendoza LH, Wang XF, Frangogiannis NG. Smad3 signaling critically regulates fibroblast phenotype and function in healing myocardial infarction. *Circulation Research*. 2010, 107:418–28.
 159. Liu RM, Desai LP. Reciprocal regulation of TGF- β and reactive oxygen species: A perverse cycle for fibrosis. *Redox Biology*. 2015, 6:565–77.
 160. El-Said NT, Mohamed EA, Taha RA. Irbesartan suppresses cardiac toxicity induced by doxorubicin via regulating the p38-MAPK/NF- κ B and TGF- β 1 pathways. *Naunyn-Schmiedeberg's Archives of Pharmacology*. 2019, 392:647–58.
 161. Kumaran C, Shivakumar K. Calcium- and superoxide anion-mediated mitogenic action of substance P on cardiac fibroblasts. *American Journal of Physiology - Heart and Circulatory Physiology*. 2002, 282:1855–62.
 162. Ivanová M, Dovinová I, Okruhlicová L, Tribulová N, Šimončíková P, Barte-Ková M, Vlkovicová J, Barancík M. Chronic cardiotoxicity of doxorubicin involves activation

- of myocardial and circulating matrix metalloproteinases in rats. *Acta Pharmacologica Sinica*. 2012, 33:459–69.
163. Fan D, Takawale A, Lee J, Kassiri Z. Cardiac fibroblasts, fibrosis and extracellular matrix remodeling in heart disease. *Fibrogenesis and Tissue Repair*. 2012, 5:1–13.
 164. Coppola C, Riccio G, Barbieri A, Monti MG, Piscopo G, Rea D, Arra C, Maurea C, Lorenzo CD, Maurea N. Antineoplastic-related cardiotoxicity, morphofunctional aspects in a murine model: Contribution of the new tool 2D-speckle tracking. *OncoTargets and Therapy*. 2016, 9:6785–94.
 165. Gambardella J, Trimarco B, Iaccarino G, Sorriento D. Cardiac nonmyocyte cell functions and crosstalks in response to cardiotoxic drugs. *Oxidative Medicine and Cellular Longevity*. 2017, 2017:1-12.
 166. Yavas G, Celik E, Yavas C, Elsurer C, Afsar RE. Spironolactone ameliorates the cardiovascular toxicity induced by concomitant trastuzumab and thoracic radiotherapy. *Reports of Practical Oncology and Radiotherapy*. 2017, 22:295–302.
 167. Spach MS, Boineau JP. Microfibrosis produces electrical load variations due to loss of side- to-side cell connections: A major mechanism of structural heart disease arrhythmias. *PACE - Pacing and Clinical Electrophysiology*. 1997, 20:397–413.
 168. Boo S, Kopecka J, Brusa D, Gazzano E, Matera L, Ghigo D, Bosia A, Riganti C. iNOS activity is necessary for the cytotoxic and immunogenic effects of doxorubicin in human colon cancer cells. *Molecular Cancer*. 2009, 8:1–18.
 169. Seddon M, Shah AM, Casadei B. Cardiomyocytes as effectors of nitric oxide signalling. *Cardiovascular Research*. 2007, 75:315–26.
 170. Wilmes V, Scheiper S, Roehr W, Niess C, Kippenberger S, Steinhorst K, Verhoff MA, Kaufenstein S. Increased inducible nitric oxide synthase (iNOS) expression in human myocardial infarction. *International Journal of Legal Medicine*. 2020, 134:575-581.
 171. Vu T, Claret FX. Trastuzumab : updated mechanisms of action and resistance in breast cancer. *Frontiers in Oncology*. 2012, 2:1–7.

CHAPTER III

Experimental work. **Exploring the effects of doxorubicin on skeletal muscle remodeling**

1. Introduction

Doxorubicin (Dox) is a highly effective antitumor agent (1); however, this drug has shown deleterious side effects in several tissues and organs (2). To date, much of the research on Dox-related toxicity has been focused on its cardiotoxic effects (3,4). Nevertheless, other organs are also targeted by Dox such as skeletal muscle (3,5). Indeed, Dox seems to accumulate in skeletal muscle promoting fiber atrophy, contributing to the development of skeletal muscle weakness and fatigue in cancer patients. The loss of muscle mass and strength negatively affects the daily living activities and increases the risk of morbidity and mortality (1,2,6).

To prevent and counteract the toxic effects of Dox on skeletal muscle, it is essential to understand the molecular mechanisms responsible for such toxicity (3,7). Emerging evidence suggests that mitochondrial dysfunction plays a key role (8), which is closely related to increased oxidative stress (9). The main site of Dox-induced ROS production occurs at oxidative phosphorylation (OXPHOS) complex I via the single electron reduction of Dox (7). An unstable semiquinone is generated and forms a redox cycle that leads to the production of superoxide anion radicals, which enhance mitochondrial dysfunction (5). Dox can also interact with cardiolipin, a phospholipid located in the inner mitochondrial membrane, impairing its function in the stabilization of OXPHOS complexes (5,7). The increase in ROS is also associated with the inhibition of protein synthesis and the acceleration of proteolysis (8). Indeed, preclinical studies showed that treatment with Dox activates all the major proteolytic systems (i.e., autophagy, calpains, caspase-3, and ubiquitin-proteasome system) in skeletal muscle (7,10). In fact, the inhibition of Dox-induced calpain activation was reported to protect against skeletal muscle atrophy (8). This Dox-related acceleration of proteolysis, as demonstrated in several studies, have shown more pronounced effects on *soleus* than in other hindlimb skeletal muscles (5,8). Dox-induced skeletal muscle impairment occurs in both fast-twitch and slow-twitch muscle fibers (11); nevertheless, slow-twitch muscle fibers (e.g., *soleus*) appear to be predominantly affected given their higher mitochondrial density when compared to fast-twitch muscle fibers (12). Additionally, Dox has been demonstrated to promote oxidative-to-glycolytic metabolic shift in skeletal muscle (13), which may be due, at least in part, to Dox-induced dysfunction of mitochondrial OXPHOS (13,14). A fiber-type shift towards an increase of glycolytic fibers, potentially renders cancer patients treated with Dox more vulnerable to muscle atrophy (15).

Aiming to add new insights on the molecular adaptations promoted by Dox in skeletal muscle, in the present study we assessed the interplay between the ubiquitin-proteasome pathway and mitophagy, and the metabolic adaptations in the *soleus* muscle from mice submitted to Dox treatment with two cumulative drug concentrations (9 and 18 mg/Kg) during three weeks.

2. Materials and Methods

2.1. Animals and experimental design

Adult male CD-1 mice were acquired from Charles River Laboratories (L'Arbresle France) and maintained in the vivarium of Institute of Biomedical Sciences Abel Salazar (ICBAS; Porto, Portugal). Following a quarantine period, mice were housed in Green Line individually ventilated cages (IVC; GM500; Tecniplast, UK), in a maximum of three mice per cage, in temperature (22 ± 2 °C) and humidity-controlled environment and a 12h light-dark cycle. Standard diet (Mucedola, Settimo, Milanese, Italy) and water were provided *ad libitum*.

Mice were divided into three groups: mice injected with saline solution (0.9% NaCl; CTRL group, n = 9); injected with Dox hydrochloride prepared in saline solution to a total cumulative dose of 9 mg/Kg (Dox 9 mg/Kg group, n = 9) and 18 mg/Kg (Dox 18 mg/Kg group, n = 5). The doses were calculated based on allometric scaling and considering the conversion factor 37 for body area surface between mice and humans, as recommended by the US Food and Drug Administration (16). The Dox cumulative dose of 9 mg/Kg and 18 mg/Kg in adult mice corresponded to ~ 51.5 mg/m² and ~ 102.9 mg/m² in humans, respectively. Both cumulative doses were much lower than the maximum lifelong doses recommended for humans (Dox maximum cumulative recommended dose is 400-550 mg/m²) (17). The doses were delivered through 6 intraperitoneal injections (i.p.) twice a week for three weeks. These administration schedules were chosen to mimic human cancer therapy that consists of multiple administrations at separated time-points. One week after the last administration, mice were anesthetized through isoflurane inhalation and then sacrificed by exsanguination. Immediately after sacrifice the *soleus* and *gastrocnemius* muscles were excised, weighed, and then divided for morphological and biochemical analysis.

The animal protocol was approved by the Portuguese Ethics Committee for Animal Experimentation, *Direção Geral de Alimentação e Veterinária* (reference number

0421/000/000/2016) and the local Committee Responsible for Animal Welfare (ORBEA) of ICBAS-UP (project number 140/2015) and performed in accordance to European Council Directive (2010/63/EU).

2.2. Morphological analysis of *soleus* muscle

Cubic pieces from *soleus* muscle were fixed with buffered paraformaldehyde 4% (v/v) by diffusion during 24 h and subsequently dehydrated with graded ethanol and included in paraffin blocks. Serial cross-sections (5 μm of thickness) of paraffin blocks were cut using a microtome and mounted on silane-coated slides. The slides were dewaxed in xylene and hydrated through graded alcohols finishing in phosphate-buffered saline solution. *Soleus* sections were stained with haematoxylin–eosin (H&E), dehydrated with graded alcohols through xylene and mounted with DPX for analysis in a photomicroscope (Zeis Phomi 3). These analyses were performed at the *Laboratório de Bioquímica e Morfologia Experimental*, Faculty of Sports from University of Porto.

2.3. *Soleus* homogenate preparation

A portion of *soleus* muscle was homogenized in the proportion of 10 mg of tissue *per* 1 mL of phosphate buffer (50 mM KH_2PO_4 pH 7.5, 0.5% Triton X-100 and 200 mM PMSF), using a Teflon pestle on a motor-driven Potter-Elvehjem glass homogenizer. The obtained samples were preserved at -80°C for subsequent analysis.

2.4. Total protein quantification

An aliquot of tissue homogenate (5 μL) was used for total protein quantification using the commercial kit *DC Protein Assay* (Bio-Rad®, Hercules, CA, USA). This kit is based on Lowry *et al* (18) assay, on which proteins react with copper in an alkaline solution, occurring the reduction of Folin reagent by the copper-treated protein, leading to the formation of a blue color with maximum absorbance at 750 nm. Hence, a calibration curve with standard solutions of bovine serum albumin (BSA) at concentrations between 0.625 and 10 mg/mL was made. Briefly, to 5 μL of samples or standards was added 25 μL of reagent A' (prepared by the addition of 1 mL of reagent A and 20 μL of reagent S) and, after 5 minutes at room temperature, 400 μL of reagent B was added. After 15 minutes at room temperature, the

absorbance was measured at 750 nm in a microplate reader (Multiskan GO, Thermo Fischer Scientific®, Northumberland, UK).

2.5. Immunoblot analysis

To evaluate the amount of target proteins in *soleus* muscle, equal amounts of protein (40 µg) from each sample were dissolved in loading buffer (0.5 M Tris-HCl pH 6.8, 4 % (w/v) SDS, 15 % (v/v) glycerol, 1 mg/mL bromophenol blue and 20 % (v/v) β-mercaptoethanol) and heated 5 minutes at 100 °C (or 50 °C in the case of Mitoprofile) and then loaded in a 12.5 % SDS-PAGE gel prepared according to Laemmli (19). The gels were run for, approximately, 45 minutes at 180 V in running buffer (250 mM glycine, 25 mM Tris, pH 8.6 and 0.1 % (w/v) SDS). The resolved proteins were transferred to a nitrocellulose membrane (Amersham™ Protran™, GE Healthcare, Germany, 0.45 µm porosity) for 2 hours at 200 mA. The transfer buffer used contained 192 mM glycine, 25 mM Tris, pH 8.3 and 20 % (v/v) methanol and the efficacy of transfer was confirmed by Ponceau S staining.

Thenceforth, membranes were blocked with 5 % (w/v) nonfat dry milk in Tris-buffered saline (TBS) with Tween 20 (TBST; 100 mM Tris, 1.5 mM NaCl, pH 8.0 and 0.05 % (v/v) Tween 20) for 1 hour with shaking at room temperature in order to avoid unspecific binding. Afterwards, the membranes were incubated with the primary antibody (rabbit monoclonal anti-APG5L/ATG5 (ab108327), mouse monoclonal anti-ATPB (ab14730), rabbit polyclonal anti-ETFDH (ab91508), rabbit polyclonal anti-GAPDH (ab9485), rabbit polyclonal anti-MURF1 (ab77577), total OXPHOS rodent WB antibody cocktail (ab110413), and rabbit monoclonal anti-PFKM (ab154804) from Abcam (Cambridge, UK), and rabbit polyclonal anti-atrogin-1 (ap2041) from ECM Biosciences (Versailles, Kentucky, USA)) diluted 1:1000 in 5 % (w/v) nonfat dry milk in TBST for 2 hours with shaking at room temperature or overnight at 4 °C. Then, membranes were washed three times (10 minutes each) with TBST to remove the unbound antibodies. Subsequently, the membranes were incubated with the appropriate secondary horseradish peroxidase-conjugated antibody (anti-mouse, anti-rabbit or anti-goat; GE Healthcare, UK), diluted 1:1000 with 5 % (w/v) nonfat dry milk in TBST, for 1 hour with shaking at room temperature. After that, the membranes were washed three times (10 minutes each) with TBST and exposed, for 2 minutes, with enhanced chemiluminescence ECL reagent (WesternBright™ ECL, advansta, CA, USA). Images were acquired using ChemiDoc XRS System (Bio-Rad®, Hercules, CA, USA).

2.6. Slot-blot assessment of carbonylated proteins

The content of carbonyl groups in proteins was evaluated according to Robinson *et al* (20) with some modifications. In brief, a certain sample homogenate volume (V) containing 40 µg of protein was mixed with 12 % (w/v) SDS (V) and 20 mM 2,4-dinitrophenylhydrazine (DNPH) prepared in 10 % (v/v) trifluoroacetic acid (2V). The reaction between carbonyl groups and DNPH leads to the formation of 2,4-dinitrophenyl (DNP) hydrazone which can be detected by immunoblotting. Next, sample mixtures were incubated in the dark at room temperature for 30 minutes. The addition of 2 M Tris with 18 % (v/v) β-mercaptoethanol (1.5 V) stopped the reaction. Two different dilutions, 3:400 and 1:200, were prepared in TBS. After this, 100 µL of each sample dilution were transferred to a nitrocellulose membrane (Amersham™ Protran™, GE Healthcare, Germany, 0.45 µm porosity) under vacuum, using a Slot-blot system. The nitrocellulose membranes were first activated by immersion on 10 % (v/v) methanol solution for 5 seconds and placed in distilled water until transference procedure. The immunodetection was performed as described above for immunoblotting. The primary antibody (mouse monoclonal anti-DNP; MAB2223, Millipore) was diluted 1:1000 in 5 % (w/v) nonfat dry milk in TTBS and incubated for 1 hour at room temperature with shaking and the second antibody (anti-rabbit IgG-Peroxidase, Amersham Pharmacia) was diluted 1:1000 with 5 % (w/v) nonfat dry milk in TBST and incubated for 30 minutes at room temperature with shaking.

2.7. Spectrophotometric activity assays

2.7.1. ATP synthase activity

The activity of ATP synthase was measured according to Simon *et al* (21). The phosphate produced by hydrolysis of ATP reacts with ammonium molybdate in the presence of reducing agents to form a blue color complex. The intensity of this complex is proportional to the concentration of phosphate in solution. Equal volumes (15 µL) from each sample were dissolved in reaction buffer (0.2 M KCl, 3 mM MgCl₂, 10 mM Tris-HCl, pH 8.4) and incubated at 30 °C for 1 minute. Then an equal volume of 0.1 M ATP was added and incubated for 1 minute at 30 °C. The reaction was stopped by the addition of 30 µL of 3 M trichloroacetic acid. After vortex, 125 µL of supernatant was mixed with 625 µL of test solution (0.37 M H₂SO₄, 0.01 M ammonium molybdate and 0.1 M ferrous sulphate) and then

incubated for 15 minutes at room temperature. In parallel, a calibration curve with standard solutions of potassium dihydrogen phosphate (KH_2PO_4) at concentrations between 0.0 and 1.9 mM was prepared. Oligomycin was used as an ATP hydrolase inhibitor. The absorbance was read at 610 nm in a microplate reader (Multiskan GO, Thermo Fischer Scientific®, Northumberland, UK). Then, the absorbance values were converted to concentration (mM) *per* minute from the equation of calibration curve and then divided by total protein to obtain the enzymatic activity values (mmol/min/mg) on each sample.

2.7.2. Citrate Synthase activity

The activity of citrate synthase (CS) was measured in *soleus* homogenates according to Coore *et al* (22). This method evaluates the presence of free thiol groups in CoASH by its reaction with 5,5'-dithiobis-(2-nitrobenzoate) (DTNB). The resulting 2-nitro-5-thiolbenzoate (TNB) anion has a strong absorption at 412 nm, which might be followed spectrophotometrically. Briefly, 10 μL from each sample were incubated with 190 μL of reaction buffer (200 mM Tris buffer pH 8.0, 10 mM acetyl-CoA, 10 mM DTNB and 0.1 % (v/v) Triton X-100) and the absorbance was measured at 412 nm for 2 minutes at 30 °C in a microplate reader (Multiskan GO, Thermo Fischer Scientific®, Northumberland, UK). Thereafter, 10 μL of 10 mM oxaloacetate (OAA) was added to each well of the microplate and absorbance was immediately measured at 412 nm for 2 minutes at 30 °C. The absorbance values were plotted against time and the difference between the second and the first measurement, in relation to the slope of the equation ($(\Delta A_{412})/\text{min}$) was divided by the extinction coefficient of TNB at 412 nm ($13.6 \text{ mM}^{-1} \cdot \text{cm}^{-1}$). Then, the absorbance values were divided by total protein to obtain the enzymatic activity values (mmol/min/mg) on each sample.

2.8. Statistical analysis

Data are presented as mean \pm standard deviation (SD) of 4-6 biological replicates for all variables. The statistical analysis was performed using a One-way ANOVA followed by the Tukey multiple comparisons post hoc test (parametric data). The level of significance was set at 5 % (p -value < 0.05). GraphPad Prism® for Windows (version 6.0) was the software used.

3. Results

3.1. Effect of Dox on mice anthropometric parameters

Dox treatment promoted a reduction of body weight on mice, only statistically significant for the cumulative dose of 18 mg/Kg ($p < 0.01$ vs. Control; Table 1). Concomitantly, the loss of *gastrocnemius* muscle mass was noticed after Dox treatment, though not statistically significant. Similarly, no significant differences were observed between groups for the ratio *gastrocnemius* mass-to-body weight. Concerning *soleus* muscle, the animals treated with Dox presented a decrease in this muscle mass, though only significant for Dox treatment with the cumulative dose of 9 mg/Kg ($p < 0.05$ vs. Control). A significant reduction of the ratio *soleus* mass-to-body weight ratio was also noticed in mice treated with 9 mg/Kg ($p < 0.05$ vs. Control). No significant differences were noticed for *soleus* mass-to-body weight following Dox treatment with 18 mg/Kg (Table 1).

Table 1. The effect of Dox treatment (9 mg/Kg and 18 mg/Kg) on body weight, *gastrocnemius* muscle mass, *soleus* muscle mass and on *gastrocnemius* mass-to-body weight and *soleus* mass-to-body weight ratios. Values are expressed as mean \pm standard deviation of $n=6$.

	Experimental groups		
	Control	Dox 9mg/Kg	Dox 18mg/Kg
Body Weight (g)	42.524 \pm 4.225	40.295 \pm 2.251	37.727 \pm 6.163 **
<i>Gastrocnemius</i> muscle mass (mg)	396.0 \pm 20.6	379.0 \pm 41.6	368.6 \pm 45.4
<i>Soleus</i> muscle mass (mg)	16.5 \pm 4.3	12.5 \pm 2.6 *	14.8 \pm 3.5
<i>Gastrocnemius</i> mass-to-body weight (mg/g)	9.368 \pm 0.829	9.394 \pm 0.728	9.846 \pm 0.720
<i>Soleus</i> mass-to-body weight (mg/g)	0.387 \pm 0.090	0.308 \pm 0.048 *	0.396 \pm 0.084

** $p < 0.01$ vs. Control and * $p < 0.05$ vs. Control

3.2. Characterization of *soleus* metabolic adaptations to Dox treatment

To unveil the molecular adaptations promoted by Dox treatment on skeletal muscle, the slow-twitch *soleus* muscle was chosen based on data from Table 1 and previous reports on the susceptibility of this muscle to chemotherapy (2,5,7,8,10). Muscle sections were

separated for morphological and biochemical analysis. Unfortunately, technical issues in the preparation of *soleus* sections made unfeasible the morphological analysis of H&E stained sections of this muscle, as can be seen in Supplemental Figure S1. Thus, the cross-sectional area of fibers was not quantified, as planned, to corroborate the occurrence of *soleus* atrophy in Dox treated mice.

The metabolic adaptations of *soleus* to Dox treatment was assessed by the analysis of the content and activity of metabolic enzymes. Data obtained highlight a higher reliance of the *soleus* on glycolysis for energetic purposes after Dox treatment given by glyceraldehyde-3-phosphate dehydrogenase (GAPDH) and phosphofructokinase 1 (PFK1) levels (Figure 5). However, whereas a significantly higher content of GAPDH was noticed in *soleus* from mice treated with Dox 9 mg/Kg and Dox 18 mg/Kg ($p < 0.01$ vs. Control), only significant higher PFK1 levels were noticed in muscle treated with Dox 18 mg/Kg. Regarding the content of ATP synthase subunit β , no significant differences between groups were noticed (Figure 5B). Similarly, no significant variations were observed for ATP synthase activity (Figure 5D), suggesting that Dox did not interfere in the muscle fiber ability to produce ATP. Nevertheless, the ratio GAPDH-to-ATP synthase subunit β levels showed significantly higher values in Dox 9 mg/Kg and Dox 18 mg/Kg treated mice ($p < 0.001$ vs. Control and $p < 0.01$ vs. Control, respectively), supporting Dox-induced metabolic remodeling towards a glycolytic phenotype.

The analysis of the content of the electron transfer flavoprotein dehydrogenase (ETFHDH), the enzyme that mediates the transfer of electrons gathered in fatty acid oxidation (FAO) to OXPHOS (23), revealed no significant differences between groups (Figure 5F), suggesting that Dox treatments did not impact FAO on *soleus* muscle.

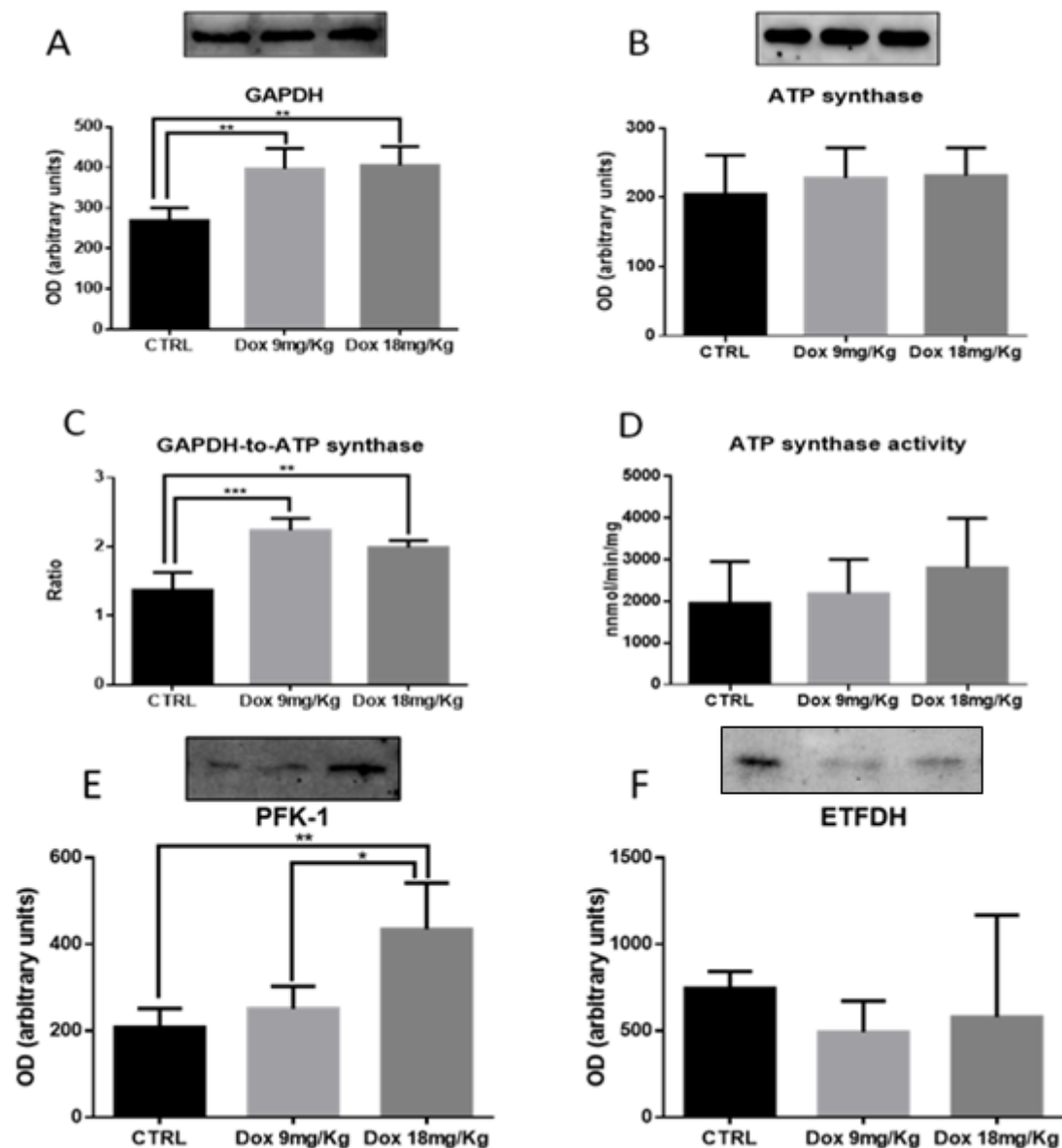


Figure 5. Effects of Dox 9mg/Kg and Dox 18mg/Kg on different molecular markers of metabolism: (A) GAPDH content; (B) ATP synthase β subunit protein content; (C) Ratio between GAPDH and ATP synthase β subunit; (D) ATP synthase activity; (E) PFK-1 content; (F) ETFDH content. Representative blots are shown above the corresponding graphics for A, B, E and F – samples were loaded in the gel one per group side-by-side. The values (mean \pm SD) are expressed in arbitrary units of optical density (OD) for A, B, E and F of n=4-6, and in nmol/min/mg for D of n=6. * p<0.05; ** p<0.01; ***p<0.001.

To better explore the effect of Dox treatments on OXPHOS adaptations, the content of specific subunits from each OXPHOS complex was measured (Figure 6). No significant differences were noticed for complex II (CII-SDHB) and complex IV (CIV-MTCO1). The analysis of complex III (CIII-UQCRC2) showed significantly higher values in the *soleus* muscle from mice treated with 18 mg/Kg Dox ($p < 0.05$ vs. Control; Figure 5B). The subunits from OXPHOS complex I (CI-NDUFB8) and complex V (CV-ATP5A) were not detected using the methodology adopted.

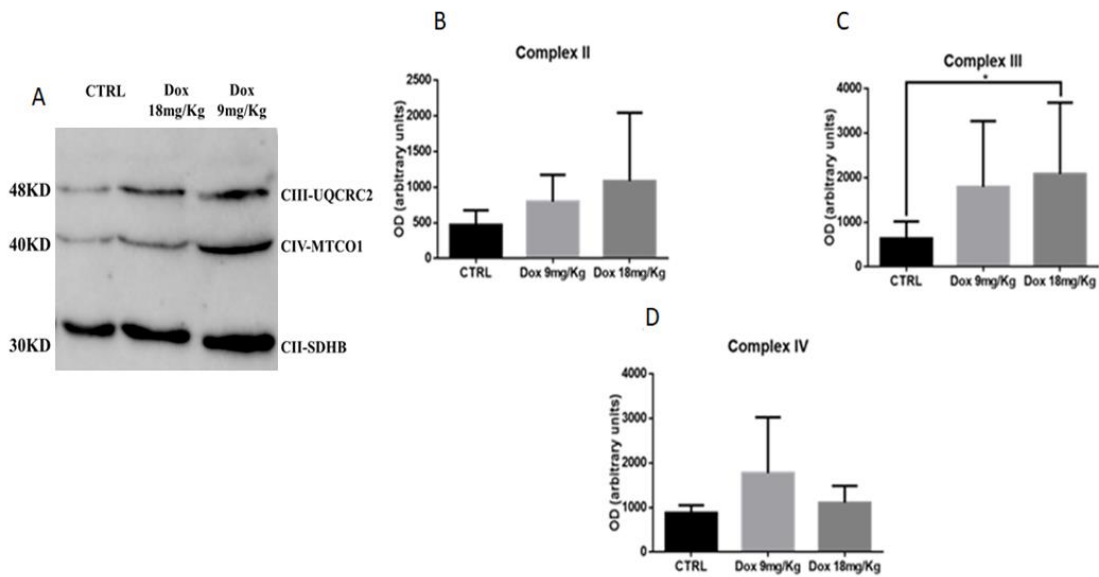


Figure 6. Effects of Dox 9mg/Kg and Dox 18mg/Kg on the levels of OXPHOS subunits. (A) Representative western blot for OXPHOS complexes subunits; (B) Expression levels of complex II, CII-SDHB, (C) complex III, CIII-UQCRC2, and (D) complex IV, CIV-COX II. The values (mean \pm SD) are expressed in arbitrary units of optical density (OD) of $n=6$.

To evaluate the impact of Dox-induced metabolic adaptations on protein susceptibility to oxidation, the content of carbonylated proteins was assessed by immunoblotting (Figure 7). The results evidenced no significant differences between groups, though a trend towards lower levels of carbonylated proteins was noticed in the *soleus* of Dox treated mice. Thus, data suggest that Dox-induced metabolic remodeling towards a glycolytic phenotype protects skeletal muscle proteome from oxidative damage (5).

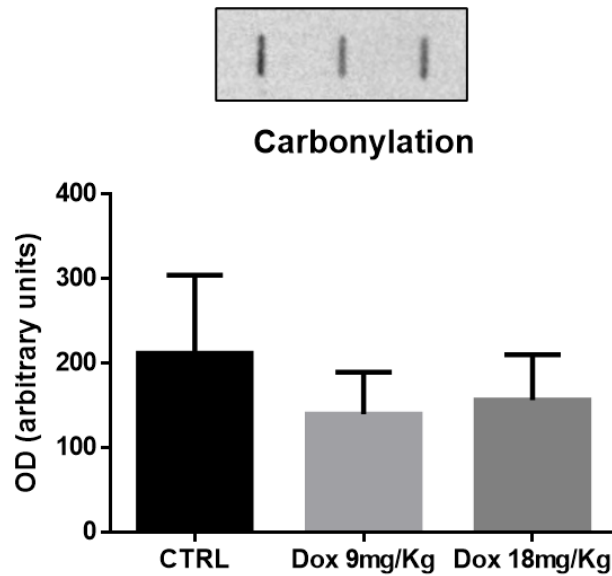


Figure 7. Effects of Dox 9mg/Kg and Dox 18mg/Kg on the protein carbonylated levels; above the graph is presented a representative image of the slot-blot obtained – samples were loaded in the gel one per group side-by-side. The values (mean \pm SD) are expressed in arbitrary units of optical density (OD) of n=6.

The activity of the Krebs cycle enzyme citrate synthase (CS), a rough marker of mitochondrial density (24), was also spectrophotometrically assessed in whole muscle extracts. No significant differences were noticed between experimental groups (Figure 8A), which suggests that the Dox treatment did not impact *soleus* mitochondrial density. To add insights on mitochondrial dynamics, the content of ATG5, a marker of mitophagy, was assessed by immunoblotting (Figure 8B). The results evidenced no significant differences between groups.

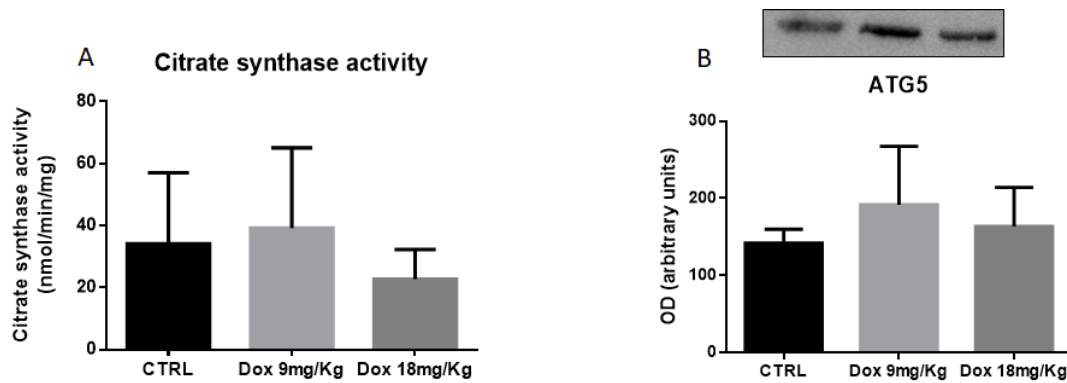


Figure 8. Effects of Dox 9mg/Kg and Dox 18mg/Kg on citrate synthase activity (A) and Atg5 levels (B). The values (mean \pm SD) are expressed in nmol/min/mg of $n=6$ for CS activity and in arbitrary units of optical density (OD) for Atg5 content of $n=6$.

3.3. The contribution of the ubiquitin-proteasome system (UPS) to Dox-induced soleus remodeling

To better understand *soleus* mass decrease promoted by Dox treatments (Table 1), the contribution of the UPS was evaluated through the assessment of the E3 ligases MURF-1 and atrogenin-1 content. Curiously, data obtained revealed no significant differences between groups (Figure 9). Thus, other proteolytic systems or changes in muscle protein synthesis might explain the decrease in *soleus* mass observed in Dox treated mice.

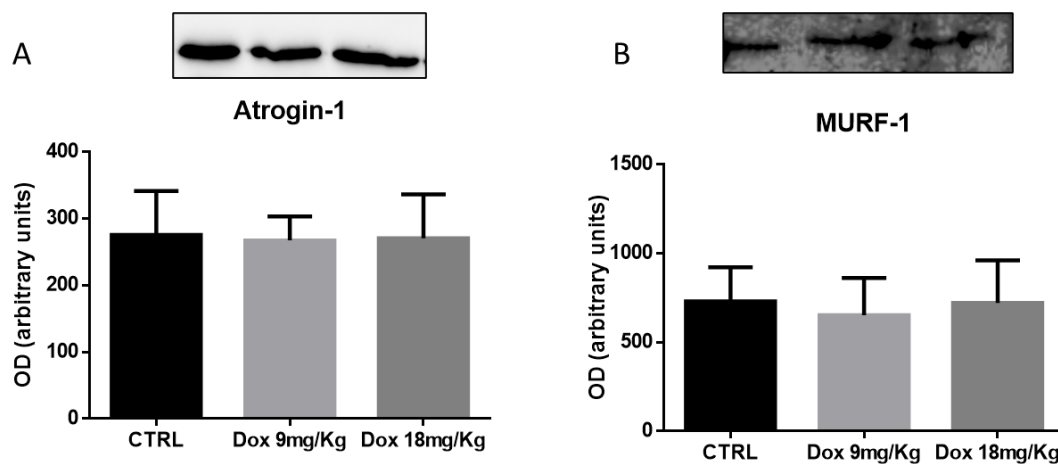


Figure 9. Effects of Dox 9mg/Kg and Dox 18mg/Kg on the content of atrogenin-1 (A) and MURF-1 (B) measured by western blotting; above each graph is presented a representative image of the western blots obtained – samples were loaded in the gel one per group side-by-side. The values (mean \pm SD) are expressed in arbitrary units of optical density (OD) of $n=6$.

4. Discussion

Dox has shown promising results in the treatment of some types of cancer such as breast cancer (1); however, this same drug has also demonstrated severe side-effects (2). Most of the studies carried out on the toxic effects induced by Dox have focused on cardiac muscle (25,26), but this drug is also toxic for other organs, being of notice its toxicity on skeletal muscle (3). Aiming to add new insights on the molecular mechanisms underlying Dox toxicity on skeletal muscle, we studied the metabolic alterations induced by Dox and related it with muscle mass regulation.

An animal model was used to assess the cumulative effect of Dox on skeletal muscle remodeling. Indeed, the use of mice for research purposes has several advantages such as their relatively small size and the little space or resources required for their maintenance. The ethical issues involved in the study of drugs in humans make mice a good alternative, particularly considering Dox toxicity (27). Moreover, several studies have successfully used mice model to study Dox toxicity (13,28). Two concentrations of Dox were used in the present study: 9 mg/Kg and 18 mg/Kg. Powers *et al* (9) showed that Dox is dose dependent cytotoxic and often results in the damage of skeletal muscles. By testing two different cumulative doses of Dox, we expected to corroborate the dose-dependent effect of Dox toxicity; however, our data do not support this hypothesis.

Our study focused on *soleus* muscle since no significant changes in *gastrocnemius* mass were observed (Table 1). Moreover, slow-twitch muscle fibers were reported to be more susceptible to Dox toxicity (8). In fact, the percentage of type I muscle fibers were reported to decrease in rats after receiving a single intraperitoneal injection of Dox (20 mg/Kg of body weight) (29), which reflects a shift towards a glycolytic phenotype. Since the *soleus* muscle mostly contains type I fibers (slow, oxidative), changes towards a glycolytic metabolism will have a more pronounced effect on this muscle when compared to *gastrocnemius* muscle (12). Our data confirmed this Dox-induced metabolic shift in the *soleus* muscle, given by the increase in the levels of GAPDH and PFK1, supporting a greater reliance of this muscle on glycolysis for energetic purposes (Figure 5). This assumption was further reinforced by the higher levels of the ratio GAPDH-to-ATP synthase subunit β . Moreover, no alterations on fatty acid oxidation were observed, given the lack of changes in the levels of ETFDH (Figure 5). FAO and OXPHOS are harbored on mitochondria, which density is high in this slow-twitch muscle, allowing a high oxidative capacity and long-term

sustain of energy demands (30). Thus, Dox-induced *soleus* metabolic remodeling towards a glycolytic phenotype was expected to be accompanied by a decrease in mitochondria density and function, a known target of this chemotherapeutic drug. In fact, it has been shown that after a single Dox injection (20 mg/Kg) the mitochondrial respiratory capacity decreases in the *soleus* muscle of rats (31,32). Nevertheless, our results of OXPHOS subunits contents and ATP synthase activity (Figures 5 and 6) refute these previous findings. Additionally, no changes in the activity of CS (Figure 8), a rough marker of mitochondrial density (33), were observed, suggesting that Dox at the therapeutic scheme used had no impact on mitochondria content in *soleus*. Biomarkers of mitochondrial biogenesis such as peroxisome proliferator-activated receptor gamma coactivator-1 α (PGC-1 α), mitochondrial transcription factor A (TFAM), mitofusins, should also be analyzed to better enlighten the contribution of mitochondrial biogenesis the Dox-induced *soleus* remodeling. In fact, we assessed the content PGC-1 α by WB, but no results were obtained. Nevertheless, it was previously demonstrated that PGC-1 α levels in the *gastrocnemius* of mice decrease after exposure to Dox (13), which may justify the change in favor of glycolytic metabolism (34).

To add insights on mitochondrial dynamics, the contribution of mitophagy to *soleus* remodeling following Dox treatment was evaluated through the assessment of Atg5. This protein is involved in the extension of the phagophore membrane in autophagic vesicles (35). However, no changes in this protein content were observed following Dox treatment (Figure 8), unlike the previously reported in rats (8).

Although OXPHOS complexes were not affected by the Dox treatments used, the significant increase of OXPHOS complex III subunit 2 (Figure 6) in mice treated with 18 mg/Kg may reveal a potential increase in ROS production. Indeed, apart from complex I, complex III has been identified as the main site of superoxide anion, and derived ROS, production within mitochondria (36). Increased mitochondrial ROS was reported in *soleus* following Dox treatment (5), and can result in the oxidative modification of proteins, which increases their susceptibility for degradation (37). In fact, the administration of Dox in rats (20 mg/Kg) was reported to increase the content of protein carbonyls in *soleus* muscle (28), unlike the observed in our study (Figure 7). The maintenance of carbonylated proteins content can be justified, at least in part, by the strong antioxidant content present in skeletal muscle fibers, such as glutathione peroxidase (GPx) (38). When proteins are irreversibly damaged, they should be eliminated to avoid fibers damage and, eventually, death (39).

Thus, the contribution of the ubiquitin-proteasome system (UPS) was evaluated, once UPS is one of the main pathways involved in protein quality control and, consequently, on the maintenance of cell homeostasis (40). The E3 ligases atrogin-1 and MURF-1 are directly involved in the regulation of skeletal muscle protein breakdown by targeting proteins for degradation (29). Indeed, after Dox administration, the levels of atrogin-1 and MURF-1 were reported to increase in rats *soleus* muscle (41). However, no changes in the content of these E3 ligases were observed in the present study (Figure 9). Despite the lesser effectiveness of glycolysis in energy production, the Dox-related higher reliance on this metabolic pathway seems to have no impact on the ATP-dependent protein degradation mediated by UPS (42). Hence, the decrease in *soleus* mass observed in mice treated with Dox does not seem to be due to muscle proteolysis, as previously suggested by Julienne *et al* (43). Other molecular pathways involved in muscle mass regulation, such as Akt/mTOR pathway, should be studied to better understand Dox-induced decrease of *soleus* mass.

In conclusion, our study shows that Dox treatment in mice promotes the remodeling of *soleus* muscle, mainly at the metabolic level. Indeed, our study revealed a metabolic adaptation towards a higher reliance on the use of glucose for energetic purposes. Unexpectedly, no changes in mitochondrial dynamics were seen; however, more molecular markers should have been evaluated, such as PGC-1 α , TFAM, mitofusins. UPS did not contribute to *soleus* remodeling. Thus, the contribution of other proteolytic systems and the Akt/mTOR signaling that control protein synthesis should be analyzed. Still, *soleus* from mouse is a challenging sample to study since the amount of protein that can be obtained is very low, which limits the choice of the molecular markers to be analyzed.

References

1. Fabris S, MacLean DA. Skeletal muscle an active compartment in the sequestering and metabolism of doxorubicin chemotherapy. *PLoS One*. 2015, 9:1–16.
2. Hochberg LM, Busekrus RB, Hydock DS. The Effects of Wheel Running on Skeletal Muscle Function during and following Doxorubicin Treatment. *Rehabilitation Oncology*. 2019, 37:114–121.
3. Dickinson JM, D'Lugos AC, Mahmood TN, Ormsby JC, Salvo L, Dedmon WL, Patel SH, Katsma MS, Mookadam F, Gonzales RJ, Hale TM, Carroll CC, Angladi SS. Exercise Protects Skeletal Muscle during Chronic Doxorubicin Administration. *Medicine and Science in Sports and Exercise*. 2017, 49:2394-2403.
4. Murabito A, Hirsch E, Ghigo A. Mechanisms of Anthracycline-Induced Cardiotoxicity: Is Mitochondrial Dysfunction the Answer? *Frontiers in Cardiovascular Medicine*. 2020, 7:1–12.
5. Doerr V, Montalvo RN, Kwon OS, Talbert EE, Hain BA, Houstoun FE, Smuder AJ. Prevention of doxorubicin-induced autophagy attenuates oxidative stress and skeletal muscle dysfunction. *Antioxidants*. 2020, 9:1–17.
6. Gibson NM, Quinn CJ, Pfannenstiel KB, Hydock DS, Hayward R. Effects of age on multidrug resistance protein expression and doxorubicin accumulation in cardiac and skeletal muscle. *Xenobiotica*. 2014, 44:472–479.
7. Powers SK, Duarte JÁ, Nguyen BL, Hyatt H. Endurance Exercise Protects Skeletal Muscle Against Both Doxorubicin-induced and Inactivity-induced Muscle Wasting. *European Journal of Physiology*. 2020, 471:441–453.
8. Smuder AJ, Kavazis AN, Min K, Powers SK. Exercise protects against doxorubicin-induced markers of autophagy signaling in skeletal muscle. *Journal of Applied Physiology*. 2011, 111:1190–1198.
9. Powers SK, Bomkamp M, Ozdemir M, Hyatt H. Mechanisms of exercise-induced preconditioning in skeletal muscles. *Redox Biology*. 2020, 35:1-8.
10. Park SS, Park HS, Jeong H, Kwak HB, No MH, Heo JW, Yoo SZ, Kim TW. Treadmill exercise ameliorates chemotherapy-induced muscle weakness and central fatigue by enhancing mitochondrial function and inhibiting apoptosis. *International Neuropsychology Journal*. 2019, 23:S32–S39.

11. Ertunc M, Sara Y, Onur R. Differential contractile impairment of fast- and slow-twitch skeletal muscles in a rat model of doxorubicin-induced congestive heart failure. *Pharmacology*. 2009, 84:240–8.
12. Bourdeau-julien I, Dutchak PA, Sephton CF. Metabolic Networks Influencing Skeletal Muscle Fiber Composition. *Frontiers in Cell and Development Biology*. 2018, 6:1-15.
13. Supriya R, Tam BT, Pei XM, Lai CW, Chan LW, Yung BY, Siu PMR. Doxorubicin Induces Inflammatory Modulation and Metabolic Dysregulation in Diabetic Skeletal Muscle. *Frontiers in Physiology*. 2016, 7:1–13.
14. Maldonado EN, Lemasters JJ. Warburg revisited: Regulation of mitochondrial metabolism by voltage-dependent anion channels in cancer cells. *Journal of Pharmacology and Experimental Therapeutics*. 2012, 342:637–641.
15. De Theije CC, Langen RCJ, Lamers WH, Gosker HR, Schols AMWJ, Köhler SE. Differential sensitivity of oxidative and glycolytic muscles to hypoxia-induced muscle atrophy. *Journal of Applied Physiology*. 2015, 118:200–11.
16. Reagan-shaw S, Nihal M, Ahmad N. Dose translation from animal to human studies revisited. *FASEB Journal*. 2019, 659–61.
17. Reis-Mendes AF, Sousa E, Bastos ML, Costa VM. The Role of the Metabolism of Anticancer Drugs in Their Induced-Cardiotoxicity. *Current Drug Metabolism*. 2015, 17:75–90.
18. Lowry OH, Rosebrough NJ, Farr AL, Randall RJ. Protein measurement with the Folin phenol reagent. *Journal of Biological Chemistry*. 1951, 193:265-275.
19. Laemmli UK. Cleavage of structural proteins during the assembly of the head of bacteriophage T4. *Nature Publishing Group*. 1970, 227:680-685.
20. Robinson CE, Keshavarzian A, Pasco DS, Frommel TO, Winship DH, Holmes WE. Determination of protein carbonyl groups by immunoblotting. *Analytical Biochemistry*. 1999, 266:48–57.
21. Simon N, Papa K, Vidal J, Boulamery A, Bruguerolle B. Circadian rhythms of oxidative phosphorylation: Effects of rotenone and melatonin on isolated rat brain mitochondria. *Chronobiology International*. 2003, 20:451–461.
22. Coore HG, Denton RM, Martin BR, Randle PJ. Regulation of adipose tissue pyruvate dehydrogenase by insulin and other hormones. *The Biochemical Journal*. 1971,

- 125:115-127.
23. Li Y, Zhu J, Hu J, Meng X, Zhang Q, Zhu K, Chen X, Chen X, Li G, Wang Z, Lu G. Functional characterization of electron-transferring flavoprotein and its dehydrogenase required for fungal development and plant infection by the rice blast fungus. *Scientific Reports*. 2016, 6:1–13.
 24. Wibom R, Hagenfeldt L, Von Döbeln U. Measurement of ATP production and respiratory chain enzyme activities in mitochondria isolated from small muscle biopsy samples. *Analytical Biochemistry*. 2002, 311:139–151.
 25. Zhou L, Xia J, Qiu X, Wang P, Jia R, Chen Y, Yang B, Dai Y. In vitro evaluation of endothelial progenitor cells from adipose tissue as potential angiogenic cell sources for bladder angiogenesis. *PLoS One*. 2015, 10:1–15.
 26. Xu X, Chen K, Kobayashi S, Timm D, Liang Q. Resveratrol attenuates doxorubicin-induced cardiomyocyte death via inhibition of p70 S6 kinase 1-mediated autophagy. *Journal of Pharmacology and Experiments Therapeutics*. 2012, 341:183–95.
 27. Perlman RL. Mouse Models of Human Disease: An Evolutionary Perspective. *Evolution, Medicine, and Public Health*. 2016, 170-176.
 28. Gilliam LAA, Lark DS, Reese LR, Torres MJ, Ryan TE, Lin C, Cathey BL, Neuffer PD. Targeted overexpression of mitochondrial catalase protects against cancer chemotherapy-induced skeletal muscle dysfunction. *American Journal of Physiology-Endocrinology and Metabolism*. 2016, 311:293–301.
 29. Hiensch AE, Bolam KA, Mijwel S, Jeneson JAL, Huitema ADR, Kranenburg O, Wall EVD, Rundqvist H, Wengstrom Y, May AM. Doxorubicin - induced skeletal muscle atrophy : Elucidating the underlying molecular pathways. *Acta Physiologica*. 2020, 229::1–18.
 30. Broker N, Broker BN. Mechanical Plasticity : Skeletal Muscle Adaptations Mechanical Plasticity : Skeletal Muscle Adaptations. *The Science Journal of the Lander College of Arts and Sciences*. 2015, 9:1-6.
 31. Gilliam LAA, Fisher-wellman KH, Lin C, Maples JM, Cathey BL, Neuffer PD. Free Radical Biology and Medicine The anticancer agent doxorubicin disrupts mitochondrial energy metabolism and redox balance in skeletal muscle. *Free Radical Biology and Medicine*. 2013, 65:988–96.
 32. Min K, Kwon OS, Smuder AJ, Wiggs MP, Sollanek K, Christou DD, Yoo JK, Hwang

- MH, Szeto HH, Kavazis NA, Powers S. Increased mitochondrial emission of reactive oxygen species and calpain activation are required for doxorubicin-induced cardiac and skeletal muscle myopathy. *Journal of Physiology*. 2004, 1–31.
33. Larsen S, Nielsen J, Hansen CN, Nielsen LB, Wibrand F, Stride N, Schroder HD, Boushel R, Helge JW, Dela F, Hey-Mogensen M. Biomarkers of mitochondrial content in skeletal muscle of healthy young human subjects. *Journal of Physiology*. 2012, 590:3349–60.
 34. Arany Z, Lebrasseur N, Morris C, Smith E, Yang W, Ma Y, Chin S, Spiegelman BM. The Transcriptional Coactivator PGC-1 β Drives the Formation of Oxidative Type IIX Fibers in Skeletal Muscle. *Cell Metabolism*. 2007, 5:35–46.
 35. Ye X, Zhou XJ, Zhang H. Exploring the role of autophagy-related gene 5 (ATG5) yields important insights into autophagy in autoimmune/autoinflammatory diseases. *Frontiers of Immunology*. 2018, 9:1–15.
 36. Bleier L, Dröse S. Superoxide generation by complex III: From mechanistic rationales to functional consequences. *Biochimica et Biophysica Acta*. 2013, 1–12.
 37. Chen C. Late-Onset Caloric Restriction Alters Skeletal Muscle Metabolism: Mechanisms from Animal and Human Studies. *Nutrition and Functional Foods for Healthy Aging*. 2017, 337–344.
 38. Powers SK, Ji LL, Kavazis AN, Jackson MJ. Reactive Oxygen Species: Impact on Skeletal Muscle. *Comprehensive Physiology*. 2011, 1:941–69.
 39. Fedorova M, Kuleva N, Hoffmann R. Reversible and irreversible modifications of skeletal muscle proteins in a rat model of acute oxidative stress. *Biochimica et Biophysica Acta - Molecular Basis of Disease*. 2009, 1792:1185–93.
 40. Lilienbaum A. Relationship between the proteasomal system and autophagy. *International Journal of Biochemistry and Molecular Biology*. 2013, 4:1–26.
 41. Kavazis AN, Smuder AJ, Powers SK. Effects of short-term endurance exercise training on acute doxorubicin-induced FoxO transcription in cardiac and skeletal muscle. *Journal of Applied Physiology*. 2014, 117:223–30.
 42. Murton AJ, Constantin D, Greenhaff PL. The involvement of the ubiquitin proteasome system in human skeletal muscle remodelling and atrophy. *Biochimica et Biophysica Acta*. 2008, 1782:730–43.
 43. Julienne CM, Dumas JF, Goupille C, Pinault M, Berri C, Collin A, Tesseraud S, Couet

C, Servais S. Cancer cachexia is associated with a decrease in skeletal muscle mitochondrial oxidative capacities without alteration of ATP production efficiency. *Journal of Cachexia, Sarcopenia and Muscle*. 2012, 3:265–275.

CHAPTER IV

Conclusion and Future Perspectives

From a general point of view, the use of Dox and trastuzumab for the treatment of cancer has been hampered by severe tissue toxicities, mainly at the level of the heart. Despite the knowledge of the activation of various signaling pathways harbored not only in cardiomyocytes but in other cell types such as cardiac progenitor cells, endothelial cells, fibroblasts, and leukocytes by these antineoplastic therapies, the molecular pathways underlying the cardiotoxic effect of the combined use of Dox and trastuzumab are still not completely understood. Preliminary studies suggest that the combination of these drugs blocks NRG-1/HER2 signaling promoting an increase in myocardial damage. Further studies are needed to increase the molecular knowledge about the cardiotoxicity induced by the combination of these drugs, envisioning to develop strategies to counteract such cardiotoxicity.

To date, most of the research about Dox-induced toxicity has focused on cardiotoxic effects; however, other organs are also affected, such as skeletal muscle. Dox appears to accumulate in skeletal muscle promoting fiber atrophy, which negatively affects the activities of daily living and increases the risk of morbidity and mortality in cancer patients treated with this drug. Indeed, the analysis of the data obtained from mice injected with Dox allowed us to conclude that this drug promotes the remodeling of *soleus* muscle, mainly at the metabolic level. In fact, our findings revealed a metabolic change in favor of glycolysis for energetic purposes. Curiously, this metabolic adaptation was not accompanied by changes in mitochondrial dynamics. Moreover, the ubiquitin-proteasome system does not seem to be responsible for the muscle mass decrease observed in treated mice. Difficulties in the management of protein amount obtained from *soleus* made unfeasible to explore the analysis of other molecular targets to substantiate our findings. Thus, in the future, it will be important to analyze the contribution of other proteolytic systems and of Akt/mTOR pathway, which is known to regulate protein synthesis in skeletal muscle. The association of Dox-induced skeletal muscle remodelling with cardiac muscle adaptations to this therapeutic will contribute to a more integrated picture of the systemic effects of Dox.

Appendix

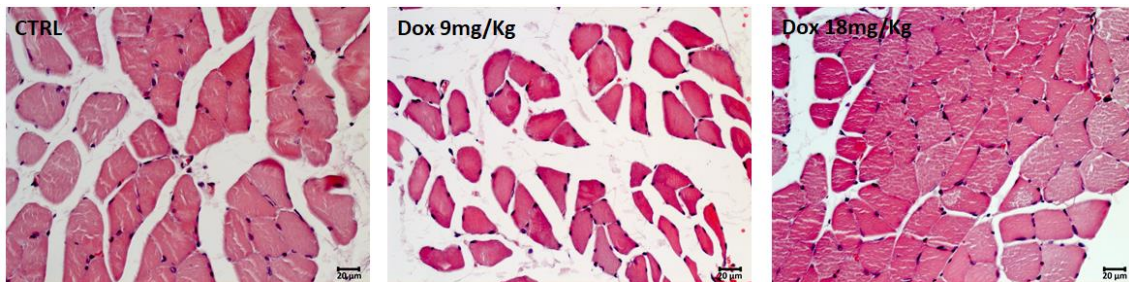


Figure S1. Representative images of hematoxylin and eosin stained *soleus* muscle sections, from CTRL (A), Dox 9 mg/Kg (B) and Dox 18 mg/Kg (C), groups. As can be seen, there are streaks in muscle fibers that appear to result from the technical procedure and not from the Dox treatments under study.

Figure S1. Representative images of hematoxylin and eosin stained *soleus* muscle sections, from CTRL (A), Dox 9 mg/Kg (B) and Dox 18 mg/Kg (C), groups. As can be seen, there are streaks in muscle fibers that appear to result from the technical procedure and not from the Dox treatments under study.

Figure S1. Representative images of hematoxylin and eosin stained *soleus* muscle sections, from CTRL (A), Dox 9 mg/Kg (B) and Dox 18 mg/Kg (C), groups. As can be seen, there are streaks in muscle fibers that appear to result from the technical procedure and not from the Dox treatments under study.

Figure S1. Representative images of hematoxylin and eosin stained *soleus* muscle sections, from CTRL (A), Dox 9 mg/Kg (B) and Dox 18 mg/Kg (C), groups. As can be seen, there are streaks in muscle fibers that appear to result from the technical procedure and not from the Dox treatments under study.